RESEARCH PAPER

Are the radiations of temperate lineages in tropical alpine ecosystems pre-adapted?

Nicolai M. Nürk[1] ⓘ   │   Florian Michling[2]   │   H. Peter Linder[3]

[1]Institute of Plant Systematics, Bayreuth Centre of Ecology and Environmental Research (BayCEER), University of Bayreuth, Bayreuth, Germany

[2]Institute of Biodiversity and Plant Systematics, Centre for Organismal Studies (COS) Heidelberg, University of Heidelberg, Heidelberg, Germany

[3]Institute of Systematic and Evolutionary Botany, University of Zürich, Zürich, Switzerland

Correspondence
Nicolai M. Nürk, Institute of Plant Systematics, Bayreuth Centre of Ecology and Environmental Research (BayCEER), University of Bayreuth, Universitätsstrasse 30, Bayreuth 95447, Germany.
Email: nicolai.nuerk@uni-bayreuth.de

Funding information
Deutsche Forschungsgemeinschaft, Grant/Award Number: NU292/1 and NU292/2

Editor: Arndt Hampe

Abstract

Aim: Tropical mountains around the world harbour an extraordinarily rich pool of plant species and are hotspots of biodiversity. Climatically, they can be zoned into montane climates at mid-altitudes and tropical alpine climates above the tree line. Around half of the tropical alpine species belong to plant lineages with a temperate ancestry, although these regions are often geographically distant. We test the hypothesis that these temperate lineages are pre-adapted to the tropical alpine climate.

Location: New World, with a focus on tropical alpine Andes.

Time period: Miocene to present.

Major taxa studied: Flowering plants.

Methods: We build multidimensional environmental models representing the full space of New World climates. We quantify the environmental similarity between the tropical alpine ecosystem and those of potential source areas, while correcting for regional differences by kernel density smoothers. Based on spatial observations of the genus *Hypericum* (St John's Wort), we quantify niche overlap and test for niche conservatism following intercontinental dispersal using density-weighted nonparametric tests. A dated species tree, biogeographical estimation, multi-optima Ornstein–Uhlenbeck models and model selection approaches are used to test for niche shifts during establishment in the tropical alpine Andes.

Results: The tropical alpine ecosystem is isolated by its climate from adjacent regions and is climatically similar to temperate lowland biomes of both hemispheres. Niche conservatism is evident in the study group, except in the tropical alpine lineage that is characterized by niche expansion and shifts in temperature optima.

Main conclusions: Our results reject the pre-adaptation hypothesis and instead suggest pronounced niche evolution during colonization of tropical alpine ecosystems. Establishment involved substantial niche shifts, mainly in temperature-related variables, and resulted in a tremendous proliferation of species in the newly invaded tropical alpine ecosystem.

KEYWORDS
Andean páramos, comparative phylogenetic analyses, global climate similarity, mountain ecology, niche shifts, temperate niche conservatism, tropical alpine

1 │ INTRODUCTION

The assembly of biotas in isolated regions has intrigued biologists over the past decades, and the relative roles of dispersal barriers and ecological suitability are still controversial. Climate constrains are thought to shape broad-scale species compositions (Crisp et al., 2009; Eiserhardt, Svenning, Baker, Couvreur, & Balslev, 2013), implying that it might be easier for plants to disperse than to evolve to new

environmental conditions (Donoghue, 2008; Merckx et al., 2015). However, the efficacy of dispersal barriers is complicated by the relative size and degree of adjacency of biomes (Donoghue & Edwards, 2014), and the ability to adapt to new climates may depend on the traits of the plants (Edwards & Donoghue, 2013). Dispersal preferred over evolution often assumes pre-adaptation to the climate conditions in the invaded environment (Antonelli, 2015), but this hypothesis has not yet been tested formally.

Tropical alpine ecosystems are ideal to test the pre-adaptation hypothesis. The world's tropical alpine ecosystem is a treeless high-elevation shrub- and grassland vegetation belt restricted to the tropics (Hedberg, 1964; Luteyn, 1999; Smith & Young, 1987). Isolated from the surrounding environment by its unique climate of high diurnal temperature fluctuations but generally cool conditions throughout the year, the ecosystem is best developed in western South America, eastern Africa and central New Guinea. Tropical alpine habitats are situated *c.* 3,000–5,000 m between the temperature-driven tree line and the nival belt (Körner & Ohsawa, 2005), and include regional vegetation types such as 'páramo' in the northern Andes, 'puna/jalca' in the central and southern Andes and 'afroalpine' or 'moorland' in East Africa (Hedberg, 1964; Smith & Young, 1987). The peculiar tropical alpine climate, with its harsh environmental conditions of diurnal freeze–thaw cycles ('summer every day and winter every night'; Hedberg, 1964), produced distinctive life-forms with convergent morphological adaptations. Most striking are caulescent rosettes, that is, the frailejónes (*Espeletia*, Asteraceae) and *Puya* (Bromeliaceae) in the Andes, giant groundsels (*Dendrosenecio*, Asteraceae) and *Lobelia* (Campanulaceae) in Africa, the tree-fern *Cyathea* (Cyatheaceae) in New Guinea and the silverswords (*Argyroxiphium*, Asteraceae) in Hawaii (Hedberg & Hedberg, 1979). Giant rosettes are among the most striking distinctions between the alpine floras of temperate and tropical latitudes (Smith, 1994).

The recruitment of temperate lineages into tropical alpine regions has contributed significantly to the current biodiversity patterns in tropical mountains (Gentry, 1982). Isolated by warm, humid conditions in the surrounding lowlands, the assembly of tropical alpine floras implied repeated dispersal over long, often intercontinental distances from source areas with a climatically similar environment (Gehrke & Linder, 2009; Sklenář, Dušková, & Balslev, 2011). Between 30 and 50% (South American Andes) and up to *c.* 70% (East African mountains) of the native tropical alpine plant species have a temperate ancestry (Gehrke & Linder, 2009; Hedberg, 1964; Luteyn, 1999; Merckx et al., 2015; Sklenář et al., 2011). The high number of plant lineages with a temperate ancestry in tropical alpine floras might be attributable to more effective establishment of species that are already adapted to the cool-climate conditions in tropical mountains, viz. establishment of pre-adapted lineages (Antonelli, 2015; Donoghue, 2008; Gizaw et al., 2016; Hedberg, 1970; Luteyn, 1999). Accordingly, this hypothesis predicts that the climate niche of tropical alpine lineages is similar to that of their temperate ancestors, especially in temperature-related niche dimensions. Here, we revisit the prediction that tropical alpine species with a temperate ancestry are conserved in the environmental niche

(temperate niche conservatism hypothesis), hence are pre-adapted to tropical alpine climates.

The tropical alpine Andean flora contains several large radiations (e.g., *Lupinus*, *Gentianella*, *Valeriana*, *Hypericum*; Madriñán, Cortés, & Richardson, 2013), all presumably seeded from northern temperate regions. In this study, we use *Hypericum* to test three hypotheses. First, Andean *Hypericum* was indeed sourced from North America, and not from southern temperate or tropical regions. Second, tropical alpine climates are most similar to those of the northern temperate ecogeographical region. Thus, we expect that adjacent tropical or nearby southern temperate regions are less similar. Third, intercontinental dispersal from North America to the tropical alpine Andes is associated with temperate niche conservatism, thus implying pre-adaptation to tropical alpine temperature regimes. Niche shifts during establishment in the tropical alpine Andes would contradict pre-adaptation, suggesting in situ adaptation to the peculiar aseasonal climates instead.

2 | MATERIAL AND METHODS

2.1 | Study group

Hypericum L. (St John's Wort, Hypericaceae) probably originated in the Eurasian Oligocene (Nürk, Uribe-Convers, Gehrke, Tank, & Blattner, 2015), and reached North America 30–20 Ma (Meseguer, Aldasoro, & Sanmartín, 2013; Nürk, Scheriau, & Madriñán, 2013), diversifying into 186 recognized species (Robson, 2012). Dispersal from North to South America resulted in a non-alpine, mostly extra-tropical East South American clade with *c.* 20 species in south-eastern Brazil, Uruguay, Paraguay and adjacent Argentina, and a tropical Andean clade comprising more than 90 species. The Andean *Hypericum* species are a prominent component of the tropical alpine flora in South America, especially in the high-elevation shrub- and grassland páramo ecosystem in the northern Andes (Luteyn, 1999). Most of the species richness in Andean *Hypericum* is tropical alpine (67 páramo species), although some species do occur at lower-elevation montane areas, resulting from secondary out-of-páramo dispersals (Nürk, Scheriau et al., 2013).

2.2 | Taxon sampling and spatial data

We sampled 104 species selected to cover the geographical range of New World *Hypericum* clades (species sampling per clade: *Triadenum*, 67%; *Myriandra*, 89%; *Trigynobrathys* sensu stricto, 36%; *Gentianoides*, 100%; *Drummondii*, 50%; Andean clade, 55%; altogether, almost 60% of the described species; Supporting Information Appendix S1, Table S1; Nürk, Scheriau et al., 2013). Species distribution data were compiled from specimens cited by Robson (2012; and references therein) and from the Global Biodiversity Information Facility (gbif.org; accessed March 2016). Occurrence data were visually cross-checked. Duplicated records, obviously erroneous locality data (coordinates of herbaria/capitals/country centre) and accessions that were outside the native species ranges or with ambiguous taxonomy (Robson, 2012) were removed using the R package dismo 1.0–22 (Hijmans, Phillips, Leathwick, & Elith, 2011; R Core Team, 2013). The final occurrence dataset

TABLE 1 Climate parameters used to understand shifts in the environmental niche (with abbreviations, the limiting range of the environmental factor, phylogenetic signal measured as Blomberg's K on the New World *Hypericum* phylogeny, variation explained per principal component axis and main contributing variables)

Parameter	Abbreviation	Limiting range	Blomberg's K
Temperature variables (°C)			
Mean annual temperature[a]	T_{mean}	Lower	.196*
Mean diurnal range[a]	$T_{rangeDay}$	Upper	.094*
Isothermality	T_{iso}	Upper	.977*
Temperature seasonality[a]	T_{seas}	Upper	1.321*
Mean maximal annual temperature	T_{max}	Upper	.378*
Mean minimal annual temperature	T_{min}	Lower	.170*
Mean minimal temperature vegetation period	T_{minVeg}	Lower	.136*
Temperature annual range	T_{range}	Upper	.957*
Mean temperature of wettest quarter[a]	T_{wet}	Upper	.227*
Mean temperature of driest quarter	T_{dry}	Upper	.114*
Mean temperature of warmest quarter	T_{warm}	Upper	.339*
Mean temperature of coldest quarter	T_{cold}	Lower	.264*
Precipitation variables (mm)			
Annual precipitation[a]	P_{ann}	Lower	.024
Precipitation of wettest month	P_{max}	Lower	.026
Precipitation of driest month	P_{min}	Lower	.113*
Precipitation seasonality[a]	P_{seas}	Upper	.108*
Precipitation of wettest quarter	P_{wet}	Lower	.022
Precipitation of driest quarter[a]	P_{dry}	Lower	.095
Precipitation of warmest quarter	P_{warm}	Lower	.033
Precipitation of coldest quarter	P_{cold}	Lower	.058
Elevation above sea level (m)	Elevation	Upper	.987*
Environmental PCA	**Variation (%)**	**Main variable**	**Blomberg's K**
Axis 1	39.24	T_{seas}, P_{ann}	.108*
Axis 2	33.37	P_{dry}, P_{seas}	.089*
Axis 3	11.47	$T_{rangeDay}$, T_{mean}	.448*

[a]Variable considered in principal components analysis (PCA). Significance level: * < .05; *p*-values adjusted with Holm's correction.

contained 5,464 point locations (median 15, range 2–905 locations/species). We extracted 19 bioclimatic variables, elevation above sea level, and the mean minimal temperature of the growing season (vegetation period; Table 1; Supporting Information Appendix S1, Table S5) from the WorldClim climate layers (Hijmans, Cameron, Parra, Jones, & Jarvis, 2005), with a spatial resolution of 30′, using raster 2.3–33 in R (Hijmans, 2015).

To correct for potentially uneven sampling, we generated two sub-datasets. The first corrects for sampling bias between species and continents by sub-sampling each species to a maximum of 15 occurrences (median 14.5, 10% fewer than five locations/species); this was used for the niche similarity test (see below, section 2.5, last paragraph). The second dataset was generated to obtain species-specific descriptors of the species' climate niche to be analysed for the niche shift analyses. To do so, we defined a 10 arcmin grid and calculated per species grid-median values based on all observations of that species in a grid cell. The grid-median values were then averaged to obtain a median per variable for the species. As the climate at the peripheries of a species range or at the peripheries of the environmental niche might differ considerably from the species' main preference (Hua & Wiens, 2013; Soberón & Nakamura, 2009) we also extracted the 5% and 95% quantiles (i.e., the 'peripheral preference', reflecting the limiting range in environmental factors; Table 1).

2.3 | Phylogenetic reconstructions and age estimation

The phylogeny was inferred from the plastid *pet*D and *trn*L loci and from nuclear encoded ITS and At1G13040 protein coding homologue (putative single-copy locus from the PPR gene family; Yuan, Liu, Marx, & Olmstead, 2009). Genomic DNA was extracted from silica-dried samples or herbarium specimens (Supporting Information Appendix S1, Table S1). Each locus was separately PCR amplified and sequenced for 94 species (for primer and PCR conditions see Supporting Information Appendix S1, Molecular marker, Table S1); for 13 additional species the DNA sequences from GenBank were collected. We also included one sample each of the early diverging lineages *Hypericum elodes* and *Hypericum calcicola* (= *Thornea calcicola*), and a representative of the sister lineage of New World *Hypericum*, *Hypericum perforatum*, to serve as outgroups in the phylogenetic and the biogeographical analyses. All newly generated sequences have been submitted to EMBL database under accession number LT904447–LT904680.

Individual loci were assembled and edited in Geneious 5.4 (Biomatters, Auckland, New Zealand) and aligned using the iterative refinement method in Mafft 6.903b (Katoh, 2005). Poorly aligned or length-variable alignment partitions were excluded with Gblocks .91b (Castresana, 2000). Gene trees were constructed to test for discordance between loci under maximum likelihood (ML) in RAxML 7.3

(Stamatakis, 2006) with the GTRCAT model, and 1,000 bootstrap replicates to evaluate clade support. Given that no supported incongruence was present, we concatenated the four loci, resulting in a 2.82 kb dataset.

Dated species trees were estimated under a relaxed clock in BEAST 1.7.5 (Drummond & Rambaut, 2007) and calibrated with three fossils (as hard minimum bounds; see Supporting Information Appendix S1) using the uncorrelated lognormal model (Drummond, Ho, Phillips, & Rambaut, 2006) and a substitution model per gene chosen via the Akaike information criterion (AIC) in MrModeltest v2.3 (Nylander, 2004). We ran four independent Markov chain Monte Carlo (MCMC) chains for 10^8 cycles, sampling every 10^4 cycle, with substitution and clock models unlinked between partitions, and setting a birth–death model that accounts for incomplete sampling as tree prior. Convergence and effective sample size (> 200) of parameters were evaluated in Tracer 1.5 (Rambaut & Drummond, 2007). The maximum clade credibility chronogram that has 95% of the highest posterior density (HPD) was calculated on a combined post-burn-in posterior sample of 20,004 trees.

2.4 | Historical biogeography and biome shift estimation

Ancestral areas for each clade were estimated to determine the number and timing of dispersal(s) to South America and to the mountain biome in the Andes. We defined 11 areas, with geographical ranges shared by two or more species and delimited by geological and climatic features (Supporting Information Appendix S1, Table S2.1). We used the distance-dependent dispersal model (M_D), implemented in BayArea 1.0.2 (Landis, Matzke, Moore, & Huelsenbeck, 2013), to estimate the joint posterior probability (pp) of ancestral areas given the tree, the distribution of species and a distance-dependent dispersal rate (denoted in geographical coordinates to modify the probability of dispersal between two areas to be inversely related to the geographical distance between them, i.e., a dispersal rate modifier). We ran two MCMC chains each with default settings for 2×10^8 cycles, sampling every 2×10^4 cycles. Posterior probabilities were averaged over the runs after discarding 25% of samples as burn-in. In addition, we evaluated the model fit of six biogeographical models using sample-size-corrected AIC (AICc) scores (Supporting Information Appendix S1, Table S3) in the R package biogeobears .2.1 (Matzke, 2012). As differences between models were minor and did not affect the biogeographical inference of Andean *Hypericum* (Supporting Information Appendix S1, Figure S1), we present and discuss estimations produced with BayArea.

We estimated the timing of the first occurrence of *Hypericum* in the montane grasslands and shrublands (MGS) biome as a proxy for the species to occur in the high-altitude Andes (and other high-altitude systems) using the settings in BayArea described above. All species were assigned to (multiple) World Wildlife Fund defined biomes (Olson et al., 2001), based on the 5,464 occurrences dataset. To adjust the dispersal rate modifier of the M_D model, multidimensional scaling was applied to a distance matrix representing a globally shared border between pairs of biomes to obtain two dimensions mimicking latitude and longitude (Supporting Information Appendix S1, Table S2.2).

2.5 | Environmental space and niche similarity tests

To estimate the similarity among New World environments, we defined 10 broad-scale ecogeographical regions delimited by geographical and floristic characteristics (Körner & Ohsawa, 2005; Smith & Young, 1987): two northern temperate ($\geq 23.437°$ N) and two southern temperate regions ($\geq 23.437°$ S), divided by elevation into 'lowland' ($\leq 1,000$ m a.s.l.) and 'montane to alpine' (1,001–5,000 m) ecogeographical regions. The Tropics (23.437° N–23.437° S) were divided by elevation into 'lowland' ($\leq 1,000$ m), 'montane' (1,001–3,000 m) and 'tropical alpine' (3,001–5,000 m) ecogeographical regions. In addition, we divided the tropical alpine region by separating the páramo (11° N–8° S, 3,001–5,000 m) from the dryer southern puna/jalca ($> 11°$ S–23.437° S, 3,001–5,000 m) ecogeographical regions (Luteyn, 1999). Likewise, we recognized three tropical montane ecogeographical regions: mountains north of, within and south of the páramo range (Supporting Information Appendix S1, Table S6). We rely on a geographical delineation of regions because it is simple and, for the objective of this study, more appropriate than approaches based on climate (Körner et al., 2016; Olson et al., 2001).

We assembled a climate dataset (30′ resolution; Hijmans et al., 2005) defined by *c.* 500,000 spatial points from the New World (60° N–40° S) generated using spatially independent sampling in raster 2.3–33 (Hijmans, 2015). To account for collinearity in the climate data, we removed the variables that had high pairwise correlation with most others (Pearson $R > .75$), retaining seven variables (Table 1). The seven variables were used to build an environmental space using principal components analysis (PCA) in ade4 1.6-2 in R (Dray & Dufour, 2007). Before ordination, the variables were ln-transformed to produce approximately equal spreads. Based on the broken-stick criterion, the first three principal component (PC) axes, which explained 84.1% of variance (Table 1), were used in the subsequent analysis. Additionally, we analysed the original climate variables individually.

We quantified the climate similarity between ecogeographical regions using the pairwise similarity metric Schoener's *D* (Schoener, 1968). As we compared climatic overlap between different regions, we corrected the similarity metric by the ratio of the kernel density distribution of the available variables (climates) and the spatial points of entities (regions) in a gridded environmental space (Broennimann et al., 2012). This framework is appropriate to compare environmental similarity between any kinds of entities (populations, species, clades or areas) that differ geographically, as it corrects for differences in the available environments between different regions (Broennimann et al., 2012). To obtain a distribution of similarity, we resampled each region independently 100 times (sampling each time 1,000 spatial points per region), while calculating Schoener's *D*. Significance was accessed under a two-sample Wilcoxon rank sum test, and *p*-values were adjusted to account for multiple testing, controlling for the family-wise error rate (Holm's correction).

Based on biogeographical and phylogenetic inference, we assigned species to three categories: North American, East South American and Andean (Supporting Information Appendix S1, Table S6). We calculated Schoener's D using the 15 occurrences/species dataset to quantify pairwise niche overlap between the North American and the East South American clade, and the Andean clade, respectively, while correcting the occurrence densities of each entity by the prevalence of the environment in its range. Also, we quantified niche expansion, a niche dynamic index that measures the niche space of the 'invasive' entity (i.e., the lineage that dispersed into a new range, here the East South American or the Andean clade) that exists only in the 'invaded' range (Guisan, Petitpierre, Broennimann, Daehler, & Kueffer, 2014). We applied quantitative density-weighted randomization tests (Warren, Glor, & Turelli, 2008) to test, firstly, whether the environmental niches of pairs of entities were identical (niche identity test). Secondly, we determined whether niches were more similar (niche conservatism) or different (niche divergence) than expected by chance, based on the available environments in the range where the invasive species do occur (similarity test). The null hypothesis (measured niche overlap between entities is explained by the available environments in the ranges) is rejected if the actual overlap between the two entities falls outside of the 95% confidence limit of the null distribution (Warren et al., 2008), after Holm's correction. Given that the outcome of the niche similarity test may be sensitive to the definition of the available background (Warren, Glor, & Turelli, 2010), we repeated the test using sequentially enlarged ranges around species occurrences defining the background (Supporting Information Appendix S1, Table S7). Analyses were done using ecospat 1.1 in R (Broennimann, Di Cola, & Guisan, 2016).

2.6 | Niche shift analysis

To test the prediction that the lineage that dispersed into the Andean tropical alpine ecosystem was climatically pre-adapted, we investigated the timing of niche evolution using comparative phylogenetics and information theory-based model selection. To do so, we define four biogeographically informed 'regime models' differing in the location and number of shifts between niche optima, where regimes are clades that possess a different niche optimum (Cressler, Butler, & King, 2015). Each model represents an alternative hypothesis, designed to compare the pattern and the timing of evolution in the climate niche, and so to differentiate between 'pre-' and in situ adaptation of tropical alpine plant lineages. The first model, M1, is a 'pre-adaptation' model, with the regime shift at the stem lineage of the most recent common ancestor (MRCA) of all South American clades. M2 is a 'South America' model, with two parallel shifts to a common regime in the two purely South America clades. M3 is a 'tropical alpine' model, with a single regime shift at the MRCA of the Andean clade. M4 contains two regime shifts, one for each South American clade (Supporting Information Appendix S1, Figure S2). We consider support for M3 and M4 to be evidence for a niche shift with dispersal and establishment in the tropical alpine region, supporting in situ adaptation.

To evaluate the different regime models, we first projected the species-specific climate values onto the New World environmental

space to obtain PC scores (axes), which are spatially (Podani & Miklós, 2002) and phylogenetically unbiased (Uyeda, Caetano, & Pennell, 2015). Then, we tested for a phylogenetic signal of the environmental variables by calculating Blomberg's K in phytools .4–5 in R (Revell, 2011) for each PC axis and single variable. All analyses used the species-specific median values and the peripheral preferences, and T_{seas} was ln-transformed to reduce right skewness. We tested for significance by comparing our observed K values against null distributions generated from 1,000 simulated datasets with values randomly assigned to tips. We considered climate variables that showed a phylogenetic signal significantly different from random after Holm's correction in the subsequent analyses.

Finally, we evaluated the four regime models in a Bayesian framework assuming heterogeneous Ornstein–Uhlenbeck (OU) models (Uyeda & Harmon, 2014) and compared model fit to the data using the Bayes factor (BF) in the R package bayou 1.0.1 (Uyeda, Eastman, & Harmon, 2014). We first established whether a Brownian motion (BM), white noise (WN) or OU model (Butler & King, 2010) fitted the data best, estimating the measurement error while calculating AICc scores in geiger 2.0 in R (Pennell et al., 2014). An OU model always returned the lowest AICc score, and so was assumed to be the best model tested (Burnham & Anderson, 2002). To produce a posterior distribution of regime model parameters, we ran in bayou two MCMC chains each for 10^6 cycles, and estimated the log marginal likelihood per regime model using eight stepping stones each run for 10^5 cycles. Estimation of the shift magnitude, θ, followed Uyeda and Harmon (2014), with a centred normal prior distribution with standard deviation equal to twice that observed in the tip data, a standard error of .5, and a probability density for a half-Cauchy distribution for α and σ^2 scaled to the mean and standard deviation of the tip data. Convergence was evaluated using the Gelman diagnostic, assuming 30% as burn-in, and interpretation of the BF followed Kass and Raftery (1995).

3 | RESULTS

3.1 | Dated phylogeny

Reconstructed phylogenetic relationships agree with previous findings (Meseguer et al., 2013; Nürk, Madriñán, Carine, Chase, & Blattner, 2013; Nürk, Scheriau et al., 2013), and major clades in the tree are highly supported (Figure 1). Estimated clade ages, which are congruent to studies using the same fossil constraints (Supporting Information Appendix S1, Table S4), indicate a crown age of New World *Hypericum* of 20.8 Ma (HPD 17.0–24.7). The monophyly of the species from the tropical Andes is strongly supported [1.00 pp, 85% bootstrap support (BS)]; we refer to this clade as the 'Andean radiation'. Within the Andean radiation (crown age 3.1 Ma, HPD 2.0–4.3), two main clades received moderate support, the 'core Páramo' (.99 pp) and the 'Páramo *affinis*' clade (.98 pp). Species from North America are placed in a grade basal to the Andean radiation. The species from SE South America also form a strongly supported clade (1.00 pp, 99 BS), with a crown age of 2.6 Ma (HPD 1.5–4.0); we refer to this as 'East South American' clade.
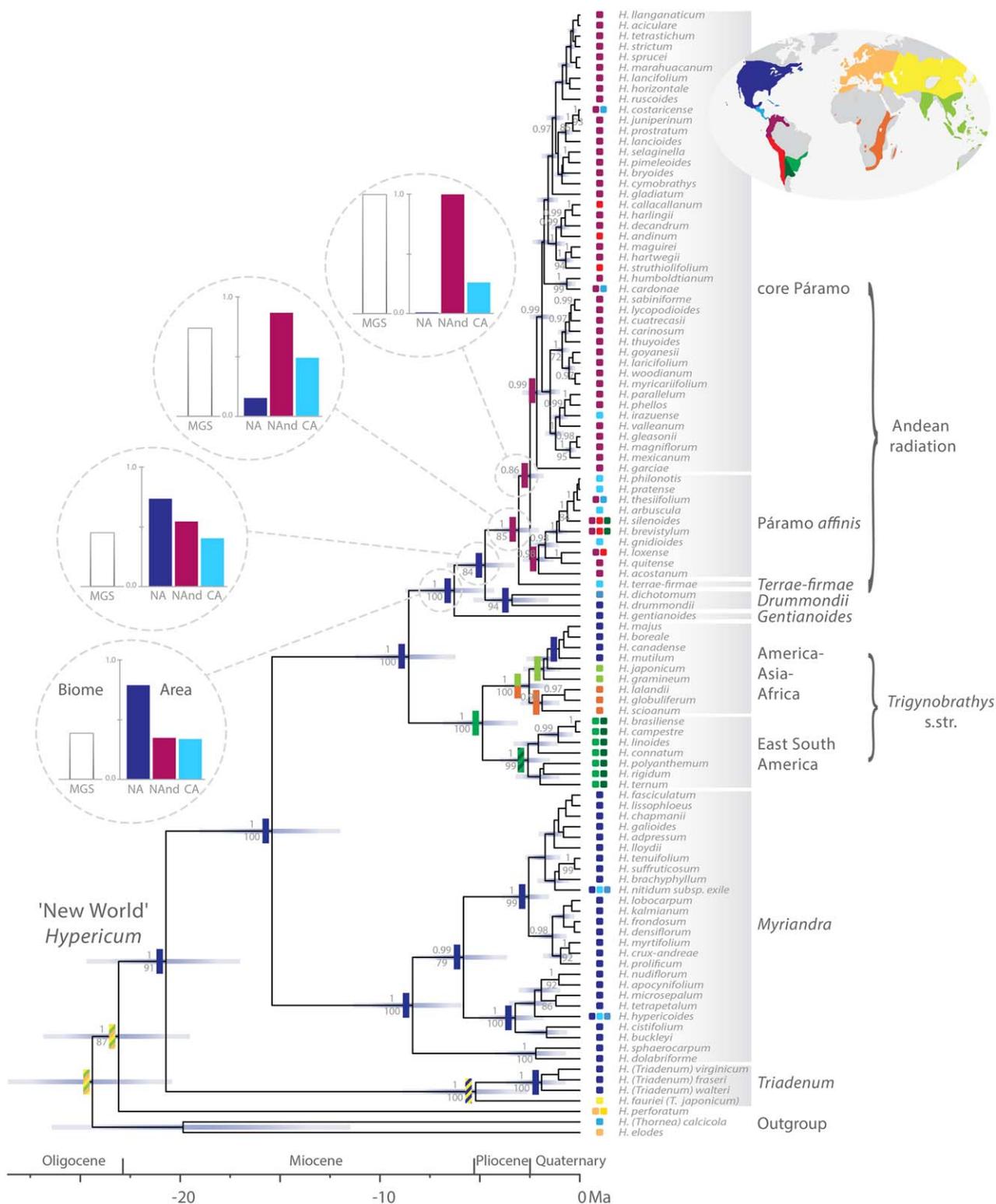
FIGURE 1 Dated species tree of 'New World' *Hypericum* detailing biogeographical history. Present distribution of species is given at the tips in the tree and best estimates of ancestral areas at internal nodes, following the colour code in the map (top right; online version). The insets on the left assign posterior probabilities of ancestral area estimations ('Area'), depicting dispersal history to the northern Andes. Also, presence in the mountain grass- and shrublands (MGS) biome ('Biome') is detailed by posterior probabilities. Clade support is given in posterior probabilities (above branches) and maximum likelihood (ML bootstrap values (below branches). CA = Central America; NA = North America; NAnd = northern Andes
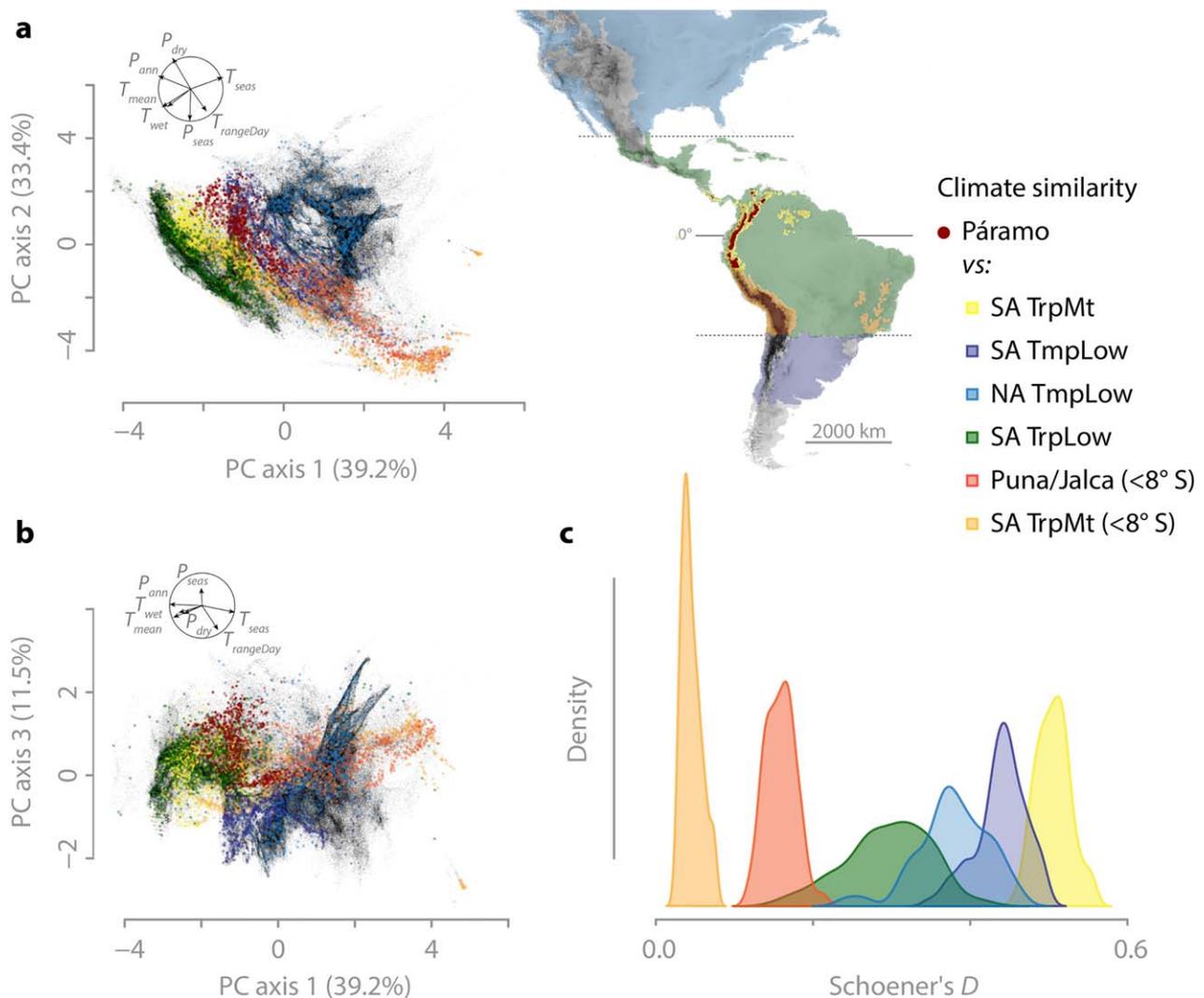
FIGURE 2 (a, b) Environmental space used to understand the climate similarity of broad-scale ecogeographical regions. Selected regions are projected onto the principal components analysis (PCA), following the colour code given in the map (top right; online version). Correlation circles indicate the contribution of climate variables to principal component (PC) axes. This environmental space was also used in the niche evolution analyses of species. (c) pairwise climate overlap (Schoener's *D*) between the tropical alpine páramo and selected regions. Low, lowland; Mt, mountain; NA, North America; Páramo, alpine between < 11° N and > 8°S; Puna/Jalca, alpine between < 8°S and > 23° S; SA = South America; Tmp = temperate; Trp = tropical

The East South American clade is sister to an American–African–Asian clade (1.00 pp, 100 BS; Figure 1).

3.2 | Biogeography and biome shifts

The ancestral area of the MRCA of New World *Hypericum* was most probably North America (Figure 1; Supporting Information Appendix S1, Figure S1, Table S4), where the lineage diversified during the Miocene. Dispersal into South America most probably occurred twice. The first dispersal, establishing the East South American clade, was estimated to have occurred to eastern South America at 1.5–4.0 Ma (.98 pp) or one node earlier at 3.1–6.9 Ma (.43 pp), depending on their ancestral area estimation (Supporting Information Appendix S1, Figure S1, Table S4). The second dispersal resulted in the Andean radiation, with a MRCA at 2.0–4.3 Ma in the northern Andes (.87 pp). The

presence of this ancestral population in Central America was supported with .47 pp (Figure 1). The MRCA of the 'core Páramo' plus 'Páramo *affinis*' clade was estimated to be distributed in the northern Andes (1.00 pp). Estimation of presence in the MGS biome revealed a congruent pattern; it was first estimated for the MRCA of the Andean radiation (.73 pp) and with high confidence for the 'core Páramo' plus 'Páramo *affinis*' clade (.99 pp; Figure 1).

3.3 | Climate similarity and niche evolution

The multidimensional environmental space obtained by PCA (Table 1), which represents the available climates in the New World, is illustrated in Figure 2a,b. Schoener's *D*, measured pairwise for ecogeographical regions on the first three axes (Figure 2c; Supporting Information Appendix S1, Table S8), shows the highest climate similarity between

TABLE 2 Niche similarity between species from North America and the Andean radiation, and North America and East South America, detailing niche overlap (Schoener's D) and niche expansion for selected parameters, and significance of niche divergence/conservatism tests

| | Andean radiation | | | | East South America | | | |
| | | | Niche similarity test | | | | Niche similarity test | |
Parameter	Niche overlap	Niche expansion	p {divergence}	p {conservatism}	Niche overlap	Niche expansion	p {divergence}	p {conservatism}
Axis 1	.618	.029	ns	ns	.628	.000	ns	*
Axis 2	.661	.069	ns	**	.226	.086	ns	**†
Axis 3	.066	.177	**†	ns	.693	.004	ns	*
Axes mean	**.448**	**.092**			**.516**	**.030**		
T_{mean}	.208	.012	ns	ns	.627	.000	ns	ns
T_{minVeg}	.247	.042	ns	ns	.451	.001	ns	*
T_{warm}	.022	.728	*†	ns	.359	.000	ns	ns
P_{min}	.204	.091	ns	ns	.344	.077	ns	*†

ns = not significant; significance level: $*p \leq .05$, $**p \leq .01$, p-values adjusted with Holm's correction; †significance independent of background.

the páramo and the tropical montane region that surrounds the páramo (i.e., 11° N–8° S; axes mean D .51), followed by the geographically more distant southern temperate lowlands (D .44). The geographically most distant North American temperate lowlands are in third position (D .38). The montane regions > 11° N and < 8° S, as well as the tropical alpine region south of the páramo (the puna/jalca ecosystems), show a notably small D of .05–.19. This pattern of climate similarity between ecogeographical regions is also evident in the analysis of individual variables (Supporting Information Appendix S1, Table S8). Páramo is most similar to the northern and southern temperate lowlands in precipitation (D P_{min} .69/.66, P_{dry} .71/.67), and differs from the puna/jalca ecosystems by these variables (D P_{min} .12, P_{dry} .12).

Pairwise niche overlap between the species distributed in North America and the species in the Andean radiation (D .45) is similar to the overlap between North American and the East South American (D .52), when averaged over the first three PC axes (Table 2). They differ, however, on axis 3, for which the overlap between the North American and East South American (D .70) is an order of magnitude larger than between North American and Andean species (D .07). Likewise, niche expansion is larger in the Andean radiation than in the East South American clade on axes 1 and 3 (Table 2). This pattern of larger niche expansion in the Andean radiation compared with the East South American clade is even more apparent in the analysis of the individual variables, especially in temperature variables (Table 2; Supporting Information Appendix S1, Tables S9.1, S9.2). Niche identity between the focal species groups is rejected for all variables (identity test, $p < .05$). The niche divergence test is significant for the Andean radiation on axis 3 and T_{warm} (similarity test, $p < .05$; all tested backgrounds; Supporting Information Appendix S1, Table S9.1). In contrast, the niche conservatism test is significant for the East South American on axes 1, 2 and 3, T_{minVeg}, P_{min} and P_{seas}, and for the Andean radiation on axis 2 only (similarity test, $p < .05$; significance is background dependent; Table 2; Supporting Information Appendix S1, Tables S9.1, 9.2).

3.4 | Niche shifts

Phylogenetic signal is significant for the three PC axes, elevation, all temperature-related variables, P_{min} and P_{seas} ($p \leq .05$; Table 1). Among these, phylogenetic signal is strongest for T_{seas} (Blomberg's K 1.32) and weakest for axis 2 (K .09). An OU model is favoured in all cases over other trait models tested, although ΔAIC to BM was < 2 for T_{iso} (Supporting Information Appendix S1, Table S10). Bayesian analysis on the timing of shifts in multi-optima OU models rejects pre-adaptation (M1) and the South America model (M2) for axis 3 and five single climate variables: T_{mean}, T_{seas}, T_{min}, T_{minVeg} and T_{warm} (Figure 3, Table 3; Supporting Information Appendix S1, Tables S10.1–3). For T_{mean}, T_{min} and T_{warm}, pre-adaptation and M2 are rejected only when the climate at the periphery of a species environmental range is considered. Pre-adaptation (but not M2) is rejected for axis 1, $T_{rangeDay}$ and T_{dry}; for the latter, only when the peripheral climate is considered. For axis 2, the remaining climate variables and elevation, the pre-adaptation hypothesis is not rejected (Supporting Information Appendix S1, Tables S10.1–4).

4 | DISCUSSION

4.1 | Tropical alpine Hypericum dispersed from North America

Biogeographical analyses failed to reject the first hypothesis, that the Andean radiation was founded by long-distance dispersal from North America (Figure 1). This dispersal to South America was probably Pliocene, 2.0–4.3 Ma, a time at which the northern Andes had already reached the necessary elevation for the development of the tropical alpine páramo (Anderson, Saylor, Shanahan, & Horton, 2015). Stepping-stone dispersal from North America to the northern Andes via the Central American mountain ranges, congruent with scenarios suggested for Halenia (von Hagen & Kadereit, 2003) and Lupinus (Drummond, Eastwood, Miotto, & Hughes, 2012), received less
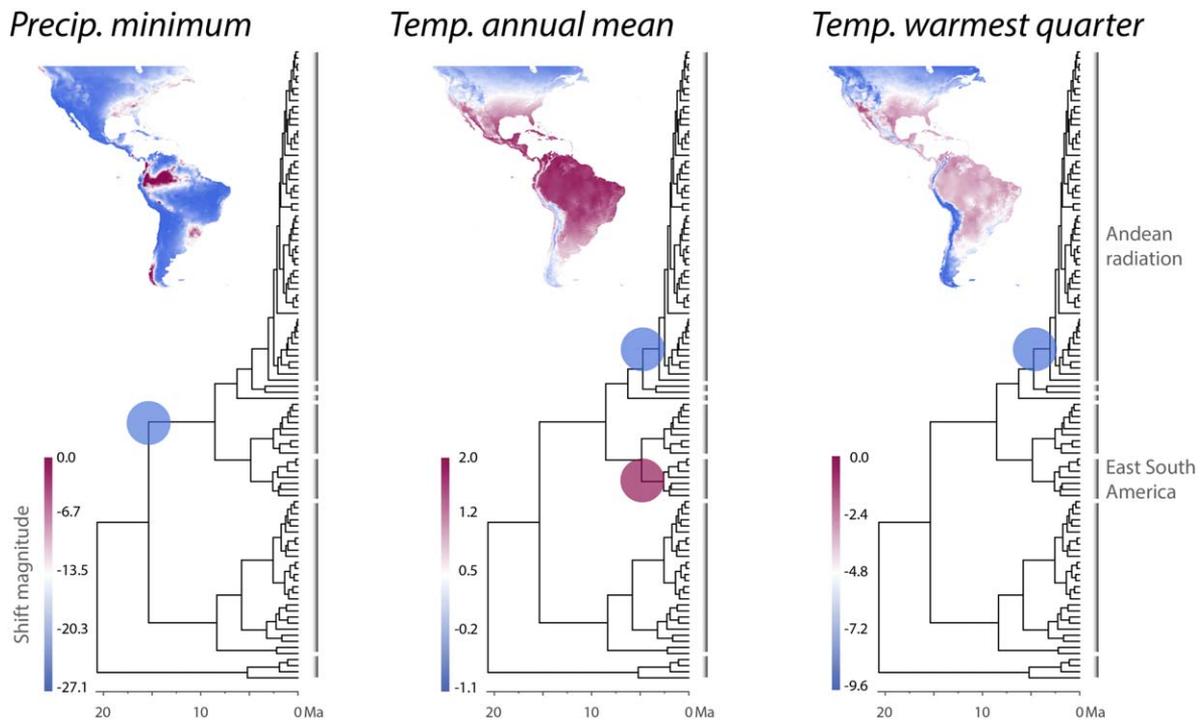
FIGURE 3 Niche shifts in 'New World' *Hypericum*, detailing the best-fitting regime model of selected climate variables and the shift magnitude to the new niche optimum (colour-coded circles on trees; online version). We interpret the shift in precipitation minimum as evidential for pre-adaptation of the Andean lineage (M1 model), the shift in annual mean temperature as in situ adaptation to divergent optima in both South American lineages (M4 model), and the shift in mean temperature of the warmest quarter as evidential for in situ adaptation in the tropical alpine ecosystem of the Andean radiation only (M3 model). The map insets (top left of the trees) depict the distribution of the respective variable in the New World. Precip. = precipitation; Temp. = temperature

support. Moreover, the biome shift estimations do not support a stepping-stone scenario via Central American mountains, as presence of *Hypericum* in the MGS biome was supported only at the crown node of the Andean radiation (Figure 1; Supporting Information Appendix S1, Figure S1, Table S4).

Assuming two dispersals from North to South America is conditional on the position of the two North American/Caribbean clades forming a grade basal to the Andean radiation (*Gentianoides* and *Drummondii*; Figure 1). In contrast, a single dispersal leading to both Andean and East South American clades implies back-dispersals of *Gentianoides* and *Drummondii* from South America to North America and the Caribbean, and so is less parsimonious than the two-dispersal model. Repeated long-distance dispersal might not be rare in *Hypericum* (Nürk & Blattner, 2010), as is also illustrated by the sister group of the East

TABLE 3 Niche shift results for selected parameters detailing the log marginal likelihood, the Bayes factors of model comparisons, and the biological interpretation of the favoured model

	Model (log marginal likelihood)			Bayes factor		
Parameter	Pre-adapted	South America	Tropical alpine	Best model over pre-adapted	Best model over South America	Biological interpretation
Axis 1	−94.8	−75.1	−76.6	39.5	0	Shift into South America (to less annual precipitation)
Axis 2	−134.8	−134.9	−134.4	.9	1.0	Pre-adapted (to greater precipitation seasonality)
Axis 3	−104.7	−103.3	−92.1	25.2	22.4	Shift into tropical alpine ecosystem (to higher temperature diurnal range)
T_{mean}	−536.7	−535.7	−533.6[a]	6.2	4.1	Shift into tropical alpine ecosystem to lower annual mean temperatures
T_{minVeg}	−538.1	−538.0	−534.8	6.5	6.5	Shift into tropical alpine ecosystem to lower minimal temperature during vegetation period
T_{warm}	−535.0	−539.1	−533.2	3.6	11.7	Shift into tropical alpine ecosystem to lower mean temperature of warmest quarter
P_{min}	−471.1	−475.6	−472.9	0	0	Pre-adapted to less precipitation during driest month

[a]South America divergent model (M4).

South American clade, which apparently dispersed from South America to North America, Africa and Asia (Figure 1). The single-dispersal scenario also entails presence of *Hypericum* in South America since the late Miocene. The palaeontological and geological record, however, suggests that, although proto-páramo conditions were met by the latest Miocene (Anderson et al., 2015), *Hypericum* established in the Andes only during the Quaternary (Hoorn et al., 2017). Thus, although a southern temperate or Central American origin cannot be rejected completely by our results, a northern temperate origin of the Andean radiation is the more likely explanation.

4.2 | The tropical alpine páramo is climatically unique

Our results reject the hypothesis that the páramo is climatically most similar to the temperate North American ecogeographical region, from which numerous lineages, including *Hypericum*, were sourced. The climatically most similar region is, maybe not surprisingly, the surrounding montane belt (Figure 2), followed by the southern temperate region. However, these generalities hide a more complex picture. Overall precipitation links the páramo to the North American and South American temperate ecogeographical regions, whereas overall temperature variables link the páramo to the surrounding tropical mountains and to the southern puna/jalca tropical alpine system. Thus, although the typical tropical alpine diurnal temperature fluctuations are shared between the páramo and the southern puna/jalca, the latter is much drier. The puna/jalca is typically xeric and has a ≥ 6-month dry season, whereas páramos are generally humid throughout the year, with frequent rain, cloud and fog (Luteyn, 1999).

It is evident that there is no potential source area in the Americas with a comparable climate to the páramo. The massive variation range in rainfall between the páramo and the puna/jalca ecosystems may act as an ecological barrier, limiting successful migration of plant lineages between these Andean tropical alpine regions (Luteyn, 1999). Likewise, lineages from the temperate South or North American regions require an adaptation to the aseasonal, diurnal temperature fluctuations, which could also act as a major migration barrier. Consequently, from where a lineage is recruited might depend on its traits (Edwards & Donoghue, 2013).

4.3 | Niche shifts in temperature optima during recruitment of tropical alpine plants

The third hypothesis, that recruitment of (north) temperate *Hypericum* into the páramo is characterized by niche conservatism, thus implying pre-adaptation to tropical alpine temperature regimes, is also rejected. This is evident from our niche comparisons, the similarity tests between North American and the Andean radiation species and the phylogeny-based niche shift tests. The niche similarity test rejects niche conservatism for the Andean radiation in temperature variables, a result opposed to significant niche conservatism in overall climate evident in the East South American species (Table 2). The hypothesis of niche conservatism in the Andean radiation could not be rejected only for axis 2 (Table 2), reflecting pre-adaptation (or indifference) of the

tropical alpine lineage to less precipitation seasonality and lower minimal precipitation. Likewise, the niche shift test rejects pre-adaptation in the Andean radiation for several temperature variables, but not for precipitation (Figure 3, Table 3). A shift in temperature seasonality, however, is expected when a lineage migrates from a temperate into a tropical region.

Under temperate niche conservatism, the shifts in annual mean and minimal temperature are not predicted. These shifts in the environmental niche during dispersal and establishment of the tropical alpine lineage illustrate that species do have to adapt to the peculiar climate conditions in the páramo. In contrast, in the East South American clade, niche conservatism in several environmental variables cannot be rejected. In the Andean radiation, however, significant niche divergence and pronounced niche expansion are evident (Table 2). The geological record further suggests that this adaptation happened only during the Quaternary (Hoorn et al., 2017). Only then did continued uplift and the Quaternary climatic variability permit the establishment of *Hypericum* in the tropical alpine ecosystem in the northern Andes.

Although we demonstrate significant niche shifts, suggesting adaptation during the establishment of lineages from the northern temperate regions in the tropical alpine ecosystem for *Hypericum*, two overriding questions remain. The first is why so many lineages are sourced from the northern temperate, rather than the southern temperate regions. We suggest that this might be related to the much larger extent of the temperate regions in the Northern compared with the Southern Hemispheres. The second question is how general these results are, and we suggest that they could apply to all lineages recruited into the tropical alpine ecosystem, because of its unique climate, stressing the importance of adaptation to the peculiar 'summer every day and winter every night' (Hedberg, 1964) climate of the tropical alpine ecosystem.

To summarize, we found evidence of pronounced shifts in temperature-related niche dimensions in the Andean radiation. This is contrasted with niche conservatism in precipitation-related dimensions; dimensions in which both source and sink area are most similar. Consequently, we reject the hypothesis that tropical alpine species are conserved in their temperate niche, thus pre-adaptation in ecologically limiting niche dimensions is rejected. We demonstrated niche divergence in temperature variables in the evolutionary history of tropical alpine species in our study system resulting, most notably, in shifts in annual mean and minimal temperatures. These results highlight the significance of adaptive evolution during establishment in the tropical alpine ecosystem.

DATA ACCESSIBILITY

All sequences generated in this study are available at ENA: www.ebi.ac.uk/ena/data/view/LT904447-LT904680.

All spatial data, species occurrences and molecular phylogenetic data are available at the Dryad repository: https://doi.org/10.5061/dryad.3cs37.

ORCID

Nicolai M. Nürk (iD) http://orcid.org/0000-0002-0471-644X

REFERENCES

Anderson, V. J., Saylor, J. E., Shanahan, T. M., & Horton, B. K. (2015). Paleoelevation records from lipid biomarkers: Application to the tropical Andes. *Geological Society of America Bulletin*, *127*, 1604–1616.

Antonelli, A. (2015). Biodiversity: Multiple origins of mountain life. *Nature*, *524*, 300–301.

Broennimann, O., Di Cola, V., & Guisan, A. (2016). *ecospat: Spatial ecology miscellaneous methods*. Vienna, Austria: R package.

Broennimann, O., Fitzpatrick, M. C., Pearman, P. B., Petitpierre, B., Pellissier, L., Yoccoz, N. G., ... Guisan, A. (2012). Measuring ecological niche overlap from occurrence and spatial environmental data. *Global Ecology and Biogeography*, *21*, 481–497.

Burnham, K. P., & Anderson, D. R. (2002). *Model selection and multimodel inference: A practical information-theoretic approach* (2nd ed.). New York, Berlin, Heidelberg: Springer Verlag.

Butler, M. A., & King, A. A. (2010). Phylogenetic comparative analysis: A modeling approach for adaptive evolution. *The American Naturalist*, *164*, 683–695.

Castresana, J. (2000). Selection of conserved blocks from multiple alignments for their use in phylogenetic analysis. *Molecular Biology and Evolution*, *17*, 540–552.

Cressler, C. E., Butler, M. A., & King, A. A. (2015). Detecting adaptive evolution in phylogenetic comparative analysis using the Ornstein-Uhlenbeck model. *Systematic Biology*, *64*, 953–968.

Crisp, M. D., Arroyo, M. T. K., Cook, L. G., Gandolfo, M. A., Jordan, G. J., McGlone, M. S., ... Linder, H. P. (2009). Phylogenetic biome conservatism on a global scale. *Nature*, *458*, 754–756.

Donoghue, M. J. (2008). A phylogenetic perspective on the distribution of plant diversity. *Proceedings of the National Academy of Sciences USA*, *105*, 11549–11555.

Donoghue, M. J., & Edwards, E. J. (2014). Biome shifts and niche evolution in plants. *Annual Review of Ecology, Evolution, and Systematics*, *45*, 547–572.

Dray, S., & Dufour, A. B. (2007). The ade4 package: Implementing the duality diagram for ecologists. *Journal of Statistical Software*, *22*, 1–20.

Drummond, A. J., & Rambaut, A. (2007). BEAST: Bayesian evolutionary analysis by sampling trees. *BMC Evolutionary Biology*, *7*, 214.

Drummond, A. J., Ho, S. Y. W., Phillips, M. J., & Rambaut, A. (2006). Relaxed phylogenetics and dating with confidence. *PLoS Biology*, *4*, 699–710.

Drummond, C. S., Eastwood, R. J., Miotto, S. T. S., & Hughes, C. E. (2012). Multiple continental radiations and correlates of diversification in *Lupinus* (Leguminosae): Testing for key innovation with incomplete taxon sampling. *Systematic Biology*, *61*, 443–460.

Edwards, E. J., & Donoghue, M. J. (2013). Is it easy to move and easy to evolve? Evolutionary accessibility and adaptation. *Journal of Experimental Botany*, *64*, 4047–4052.

Eiserhardt, W. L., Svenning, J.-C., Baker, W. J., Couvreur, T. L. P., & Balslev, H. (2013). Dispersal and niche evolution jointly shape the geographic turnover of phylogenetic clades across continents. *Scientific Reports*, *3*, 1164.

Gehrke, B., & Linder, H. P. (2009). The scramble for Africa: Pan-temperate elements on the African high mountains. *Proceedings of the Royal Society B: Biological Sciences*, *276*, 2657–2665.

Gentry, A. H. (1982). Neotropical floristic diversity: Phytogeographical connections between Central and South America, Pleistocene climatic fluctuations, or an accident of the Andean orogeny? *Annals of the Missouri Botanical Garden*, *69*, 557–593.

Gizaw, A., Brochmann, C., Nemomissa, S., Wondimu, T., Masao, C. A., Tusiime, F. M., ... Dimitrov, D. (2016). Colonization and diversification in the African 'sky islands': Insights from fossil-calibrated molecular dating of *Lychnis* (Caryophyllaceae). *New Phytologist*, *211*, 719–734.

Guisan, A., Petitpierre, B., Broennimann, O., Daehler, C., & Kueffer, C. (2014). Unifying niche shift studies: Insights from biological invasions. *Trends in Ecology and Evolution*, *29*, 260–269.

Hedberg, I., & Hedberg, O. (1979). Tropical-alpine life-forms of vascular plants. *Oikos*, *33*, 297–307.

Hedberg, O. (1964). Features of afroalpine plant ecology; avec un résumé en français. *Acta Phytogeographica Suecica*, *49*, 1–144.

Hedberg, O. (1970). Evolution of the afroalpine flora. *Biotropica*, *2*, 16–23.

Hijmans, R. J. (2015). *raster: Geographic data analysis and modeling*. Vienna, Austria: R package.

Hijmans, R. J., Phillips, S., Leathwick, J., & Elith, J. (2011). *dismo: Species distribution modeling*. Vienna, Austria: R package.

Hijmans, R. J., Cameron, S. E., Parra, J. L., Jones, P. G., & Jarvis, A. (2005). Very high resolution interpolated climate surfaces for global land areas. *International Journal of Climatology*, *25*, 1965–1978.

Hoorn, C., Bogotá-A, G. R., Romero-Baez, M., Lammertsma, E. I., Flantua, S. G. A., Dantas, E. L., ... Chemale, F. Jr. (2017). The Amazon at sea: Onset and stages of the Amazon River from a marine record, with special reference to Neogene plant turnover in the drainage basin. *Global and Planetary Change*, *153*, 51–65.

Hua, X., & Wiens, J. J. (2013). How does climate influence speciation? *The American Naturalist*, *182*, 1–12.

Kass, R. E., & Raftery, A. E. (1995). Bayes factors. *Journal of the American Statistical Association*, *90*, 773–795.

Katoh, K. (2005). MAFFT version 5: Improvement in accuracy of multiple sequence alignment. *Nucleic Acids Research*, *33*, 511–518.

Körner, C., & Ohsawa, M. (2005). Mountain systems. In Millennium Ecosystem Assessment (Ed.), *Current state and trends: Findings of the condition and trends working group* (pp. 681–716). Washington, DC: Island Press.

Körner, C., Jetz, W., Paulsen, J., Payne, D., Rudmann-Maurer, K., & Spehn, E. (2016). A global inventory of mountains for bio-geographical applications. *Alpine Botany*, *127*, 1–15.

Landis, M. J., Matzke, N. J., Moore, B. R., & Huelsenbeck, J. P. (2013). Bayesian analysis of biogeography when the number of areas is large. *Systematic Biology*, *62*, 789–804.

Luteyn, J. L. (1999). *Páramos: A checklist of plant diversity, geographical distribution, and botanical literature*. New York, NY: Scientific Publications Department New York Botanical Garden.

Madriñán, S., Cortés, A. J., & Richardson, J. E. (2013). Páramo is the world's fastest evolving and coolest biodiversity hotspot. *Frontiers in Genetics*, *4*, 192.

Matzke, N. J. (2012). Founder-event speciation in BioGeoBEARS package dramatically improves likelihoods and alters parameter inference in

dispersal–extinction–cladogenesis (DEC) analyses. *Frontiers of Biogeography*, *4*, 210.

Merckx, V. S. F. T., Hendriks, K. P., Beentjes, K. K., Mennes, C. B., Becking, L. E., Peijnenburg, K. T. C. A., . . . Schilthuizen, M. (2015). Evolution of endemism on a young tropical mountain. *Nature*, *524*, 347–350.

Meseguer, A. S., Aldasoro, J. J., & Sanmartín, I. (2013). Bayesian inference of phylogeny, morphology and range evolution reveals a complex evolutionary history in St. John's wort (*Hypericum*). *Molecular Phylogenetics and Evolution*, *67*, 379–403.

Nürk, N. M., & Blattner, F. R. (2010). Cladistic analysis of morphological characters in *Hypericum* (Hypericaceae). *Taxon*, *59*, 1495–1507.

Nürk, N. M., Madriñán, S., Carine, M. A., Chase, M. W., & Blattner, F. R. (2013). Molecular phylogenetics and morphological evolution of St. John's wort (*Hypericum*; Hypericaceae). *Molecular Phylogenetics and Evolution*, *66*, 1–16.

Nürk, N. M., Scheriau, C., & Madriñán, S. (2013). Explosive radiation in high Andean *Hypericum*—Rates of diversification among New World lineages. *Frontiers in Genetics*, *4*, 175.

Nürk, N. M., Uribe-Convers, S., Gehrke, B., Tank, D. C., & Blattner, F. R. (2015). Oligocene niche shift, Miocene diversification – Cold tolerance and accelerated speciation rates in the St. John's Worts (*Hypericum*, Hypericaceae). *BMC Evolutionary Biology*, *15*, 80.

Nylander, J. A. A. (2004). *MrModeltest v2*. Program distributed by the author. Uppsala, Sweden: Evolutionary Biology Centre, Uppsala University.

Olson, D. M., Dinerstein, E., Wikramanayake, E. D., Burgess, N. D., Powell, G. V. N., Underwood, E. C., . . . Kassem, K. R. (2001). Terrestrial ecoregions of the world: A new map of life on earth. *BioScience*, *51*, 933–938.

Pennell, M. W., Eastman, J. M., Slater, G. J., Brown, J. W., Uyeda, J. C., FitzJohn, R. G., . . . Harmon, L. J. (2014). geiger v2.0: An expanded suite of methods for fitting macroevolutionary models to phylogenetic trees. *Bioinformatics*, *30*, 2216–2218.

Podani, J., & Miklós, I. (2002). Resemblance coefficients and the horseshoe effect in principal coordinates analysis. *Ecology*, *83*, 3331–3343.

R Development Core Team. (2013). R: A language and environment for statistical computing. R Foundation for Statistical Computing, Vienna, Austria. Retrieved from http://www.R-project.org

Rambaut, A., & Drummond, A. J. (2007). *Tracer v1.4*. Retrieved from http://beast.bio.ed.ac.uk/Tracer.

Revell, L. J. (2011). phytools: An R package for phylogenetic comparative biology (and other things). *Methods in Ecology and Evolution*, *3*, 217–223.

Robson, N. K. B. (2012). Studies in the genus *Hypericum* L. (Hypericaceae) 9. Addenda, corrigenda, keys, lists and general discussion. *Phytotaxa*, *72*, 1–111.

Schoener, T. W. (1968). The Anolis lizards of Bimini: Resource partitioning in a complex fauna. *Ecology*, *49*, 704–726.

Sklenář, P., Dušková, E., &., & Balslev, H. (2011). Tropical and temperate: Evolutionary history of páramo flora. *The Botanical Review*, *77*, 71–108.

Smith, A. P. (1994). Introduction to tropical alpine vegetation. In W.P. Rundel, A.P. Smith, & F.C. Meinzer (Eds.), *Tropical alpine environments – Plant form and function* (pp. 1–20). Cambridge, U.K.: Cambridge University Press.

Smith, A. P., & Young, T. P. (1987). Tropical alpine plant ecology. *Annual Review of Ecology, Evolution, and Systematics*, *18*, 137–158.

Soberón, J., & Nakamura, M. (2009). Niches and distributional areas: Concepts, methods, and assumptions. *Proceedings of the National Academy of Sciences USA*, *106*, 19644–19650.

Stamatakis, A. (2006). RAxML-VI-HPC: Maximum likelihood-based phylogenetic analyses with thousands of taxa and mixed models. *Bioinformatics*, *22*, 2688–2690.

Uyeda, J. C., & Harmon, L. J. (2014). A novel Bayesian method for inferring and interpreting the dynamics of adaptive landscapes from phylogenetic comparative data. *Systematic Biology*, *63*, 902–918.

Uyeda, J. C., Caetano, D. S., & Pennell, M. W. (2015). Comparative analysis of principal components can be misleading. *Systematic Biology*, *64*, 677–689.

Uyeda, J. C., Eastman, J., & Harmon, L. J. (2014). *bayou: Bayesian fitting of Ornstein-Uhlenbeck models to phylogenies*. Vienna, Austria: R package.

von Hagen, K. B., & Kadereit, J. W. (2003). The diversification of *Halenia* (Gentianaceae): Ecological opportunity versus key innovation. *Evolution*, *57*, 2507–2518.

Warren, D. L., Glor, R. E., & Turelli, M. (2008). Environmental niche equivalency versus conservatism: Quantitative approaches to niche evolution. *Evolution*, *62*, 2868–2883.

Warren, D. L., Glor, R. E., & Turelli, M. (2010). ENMTools: A toolbox for comparative studies of environmental niche models. *Ecography*, *33*, 607–661.

Yuan, Y. W., Liu, C., Marx, H. E., & Olmstead, R. G. (2009). The pentatricopeptide repeat (PPR) gene family, a tremendous resource for plant phylogenetic studies. *New Phytologist*, *182*, 272–283.

BIOSKETCHES

NICOLAI M. NÜRK is interested in plant systematics and macroevolution, studying the disparity of species' traits and the associated impact on biodiversity, taking a spatio-temporal perspective.

FLORIAN MICHLING is researching phylogeographical patterns in European key conservation species for a PhD thesis, and is also developing quantitative hypothesis tests.

H. PETER LINDER is interested in the systematics of Restionaceae and danthonioid grasses, in the biogeographical pattern in the Southern Hemisphere and, in particular, in the Cape flora, as well as the assembly of tropical alpine floras.

SUPPORTING INFORMATION

Additional Supporting Information may be found online in the supporting information tab for this article.

Supplementary data to

Are the radiations of temperate lineages in tropical alpine ecosystems pre-adapted?

Nicolai M. Nürk, Florian Michling & H. Peter Linder

Global Ecology and Biogeography

The following supporting information is available for this article:

1. **Voucher**: Table S1.
2. **Molecular marker**: information on sequenced loci, primer, and PCR conditions.
3. **Age estimation**: information on fossil constrains and secondary calibrations.
4. **Biogeography and biome analyses**: BayArea M_D: Table S2.1 (areas), Table 2.2 (biomes); model comparison in biogeobears: Table S3, Figure S1; summary statistics: Table S4 (incl. node support & age estimates for clades),
5. **Environmental space and niche similarity tests:** Definition of growing seasons: Table S5; Definition of entities (species, areas): Table S6; background definitions used in the niche similarity tests: Table S7; Results of pairwise similarity analyses of areas: Tables S8; Results of niche similarity tests (species): Tables S9.1, S92;
6. **Niche shift analysis**: Definition of regime models analyzed with bayou: Figure S2; Results summary of phylogenetic niche shift analyses (Blombergg's K, model fit; niche shift): Tables S10.1–S10.4.
7. **References SI**

1. Voucher

Table S1. Species included in the study with information on herbarium specimen, clade assignment, area code used in the biogeographic analysis, and molecular marker with accession number.

Taxon	Specimen	Clade	Area	*pet*D	*trn*L	ITS	AtG13040
% Coverage				60	83	98	40
Alignment [*bp*]				1068	408	624	720
H. aciculare Kunth	Quizhepe & Lægaard 36 (BM)	core Páramo	H	LT904551	—	HG004649	—
H. acostanum N.Robson	Harling & Andersson 22231 (BM)	Páramo *affinis*	H	LT904552	—	LT904641	—
H. adpressum W.P.C.Barton	Crockett H-105 (UGA)	*Myriandra*	E	LT904553	—	AY555865.2	LT904447
H. andinum Gleason	Solomon 16104 (BM)	core Páramo	I	LT904554	LT904487	HG004725	—

Taxon (continued)	Specimen	Clade	Area	petD	trnL	ITS	AtG13040
H. apocynifolium Small	Crockett H-82 (UGA)	*Myriandra*	E	LT904555	—	AY555883.2	LT904448
H. arbuscula Stanley & Steyerm.	Hernández & Chacón 544 (BM)	Páramo *affinis*	F	LT904556	—	HG004734	—
H. boreale (Britton) Bickn.	Sanchez 62 (MA)	Am-As-Af	E	LT904557	—	KC709374	—
H. brachyphyllum (Spach) Steud.	Crockett H32ITS (UGA)	*Myriandra*	E	—	—	AY555870.2	—
H. brasiliense Choisy	Al Gentry & Solomon 44755 (BM)	East S. America	JK	LT904558	—	HG004770	—
H. brevistylum Choisy	Solomon 15221 (BM)	Páramo *affinis*	HIK	LT904559	LT904488	HG004740	—
H. bryoides Gleason	Nürk et al. 626 (ANDES, BM)	core Páramo	H	LT904560	LT904489	LT904642	LT904449
H. buckleyi M.A.Curtis	Crockett H-171 (UGA)	*Myriandra*	E	LT904561	—	LT904643	—
H. calcicola (Standl. & Steyerm.) Breedlove & E.M.McClint.	Breedlove & Thorne 21104 (BM)	outgroup	F	LT904637	LT904547	LT904679	—
H. callacallanum N.Robson	Colin Hughes 3109 (B, BM, MOL, Z)	core Páramo	I	LT904562	LT904490	HG004727	LT904450
H. campestre subsp. *campestre* Cham. & Schltdl.	Kummrow & Silva 3245 (BM)	East S. America	JK	LT904563	LT904491	HG004771	—
H. canadense L.	Crockett 19 (UGA)	Am-As-Af	E	—	—	HE653433	—
H. cardonae Cuatrec.	Nürk & Atchison 528 (ANDES, BM)	core Páramo	FH	LT904564	LT904492	HG004690	LT904451
H. carinosum R.Keller	Nürk et al. 642 (ANDES, BM)	core Páramo	H	LT904565	LT904493	LT904644	LT904452
H. chapmanii W.P.Adams	Crockett H31ITS (UGA)	*Myriandra*	E	—	—	AY555869.2	—
H. cistifolium Lam.	Crockett H43ITS (UGA)	*Myriandra*	E	—	—	AY555881.2	—
H. connatum Lam.	Serrano et al. 6893 (BM)	East S. America	JK	LT904566	LT904494	HG004774	—
H. costaricense N.Robson	Davidse 24985 (BM)	core Páramo	FH	LT904567	LT904495	HG004684	—
H. crux_andreae (L.) Crantz	Crockett H36ITS (UGA)	*Myriandra*	E	—	—	AY555874.2	—
H. cuatrecasii Gleason	Nürk et al. 609 (ANDES, BM)	core Páramo	H	LT904568	LT904496	LT904645	LT904453
H. cymobrathys N.Robson	Nürk & Atchison 562 (ANDES, BM)	core Páramo	H	LT904569	LT904497	LT904646	LT904454
H. decandrum Turcz.	Nürk & Atchison 664 (ANDES, BM)	core Páramo	H	LT904570	LT904498	LT904647	LT904455
H. densiflorum Pursh	Crockett 172 (UGA)	*Myriandra*	E	LT904571	—	AY555886	—
H. dichotomum Lam.	Thompson 11251 (BM)	*Drummondii*	G	LT904572	LT904499	HG004760	—
H. dolabriforme Vent.	Crockett H-170 (UGA)	*Myriandra*	E	LT904573	—	AY555889	—
H. drummondii (Grev. & Hook.) Torr. & A.Gray	Crockett H-176 (UGA)	*Drummondii*	E	—	—	LT904648	—
H. elodes L.	Scheriau Hyp0568 (HEID)	outgroup	B	LT904574	LT904500	LT904649	—
H. fasciculatum Lam.	Crockett H30ITS (UGA)	*Myriandra*	E	—	—	AY555868.2	—
H. fauriei (Blume) Makino	Nürk 455 (GAT)	*Triadenum*	C	LT904638	LT904549	HE653665	—
H. fraseri (Spach) Gleason	Hill 17290 (GH)	*Triadenum*	E	—	LT904548	HE653663	—
H. frondosum Michx.	Crockett H-165 (UGA)	*Myriandra*	E	LT904575	—	AY555887	—
H. galioides Lam.	Crockett H26ITS (UGA)	*Myriandra*	E	—	—	AY555864.2	—
H. garciae Pierce	Nürk et al. 629 (ANDES, BM)	core Páramo	H	LT904576	LT904501	LT904650	LT904456
H. gentianoides (L.) Britton, Sterns & Poggenb.	Nürk 457 (GAT)	*Gentianoides*	E	LT904577	LT904502	—	—
H. gladiatum N.Robson	Nürk & Atchison 579 (ANDES, BM)	core Páramo	H	LT904578	LT904503	LT904651	LT904457

Taxon (continued)	Specimen	Clade	Area	*petD*	*trnL*	ITS	AtG13040
H. gleasonii N.Robson	Nürk & Atchison 561 (ANDES, BM)	core Páramo	H	LT904579	LT904504	LT904652	LT904458
H. globuliferum R.Keller	Gehrke 246 (Z)	Am-As-Af	A	LT904580	—	LT904653	—
H. gnidioides Seem.	Hamilton et al. 885 (BM)	Páramo *affinis*	F	LT904581	LT904505	HG004738	—
H. goyanesii Cuatrec.	Nürk & Atchison 495 (ANDES, BM)	core Páramo	H	LT904582	LT904506	LT904654	LT904459
H. gramineum G.Forst.	CHR 513231 (in: Heenan 2008)	Am-As-Af	D	—	—	EU352256	—
H. harlingii N.Robson	Øllgaard et al. 90595 (BM)	core Páramo	H	LT904583	LT904507	HG004729	—
H. hartwegii Benth.	Jørgensen et al. 1246 (BM)	core Páramo	H	LT904584	—	HG004731	—
H. horizontale N.Robson	Nürk et al. 615 (ANDES, BM)	core Páramo	H	LT904585	LT904508	LT904655	LT904460
H. humboldtianum Steud.	Nürk & Atchison 659 (ANDES, BM)	core Páramo	H	LT904586	LT904509	LT904656	LT904461
H. hypericoides subsp. *hypericoides* (L.) Crantz	Proctor 30665 (BM)	*Myriandra*	EFG	LT904587	—	HG004779	—
H. irazuense Kunze ex N.Robson	Garwood et al. 316 (BM)	core Páramo	F	LT904588	—	HG004733	—
H. japonicum Thunb.	Masuda 3360 (KYO!)	Am-As-Af	D	LT904589	LT904510	HE653512	—
H. juniperinum Kunth	Nürk & Atchison 536 (ANDES, BM)	core Páramo	H	LT904590	LT904511	LT904657	LT904462
H. kalmianum L.	Nürk 397 (GAT)	*Myriandra*	E	LT904591	LT904512	HG004780	—
H. lalandii Choisy	Gehrke BG207 (Z)	Am-As-Af	A	LT904592	LT904513	LT904658	—
H. lancifolium Gleason	Nürk & Atchison 580 (ANDES, BM)	core Páramo	H	LT904593	LT904514	HG004682	LT904463
H. lancioides subsp. *congestiflorum* Cuatrec.	Nürk et al. 643 (ANDES, BM)	core Páramo	H	LT904594	LT904515	LT904659	LT904464
H. laricifolium Juss.	Nürk & Atchison 656 (ANDES, BM)	core Páramo	HI	LT904595	LT904516	LT904660	LT904465
H. linoides A.St.-Hil.	Sobral s.n. (2007) (BM)	East S. America	JK	—	—	HG004772	—
H. lissophloeus W.P.Adams	Crockett H-125 (UGA)	*Myriandra*	E	LT904596	LT904517	AY555885	LT904466
H. llanganaticum N.Robson	Øllgaard et al. 38628 (BM)	core Páramo	H	LT904597	—	HG004650	—
H. lloydii (Svenson) W.P.Adams	Crockett 1 (UGA)	*Myriandra*	E	LT904598	LT904518	AY555867.2	—
H. lobocarpum Gatt.	Crockett H38ITS (UGA)	*Myriandra*	E	—	—	AY555876.2	—
H. loxense subsp. *loxense* Benth.	Jørgensen et al. 1351 (BM)	Páramo *affinis*	HI	LT904599	—	HG004735	—
H. lycopodioides Triana & Planch.	Nürk & Atchison 557 (ANDES, BM)	core Páramo	H	LT904600	LT904519	HG004715	LT904467
H. magniflorum Cuatrec.	Cleef 4743 (BM)	core Páramo	H	LT904601	—	HG004751	—
H. maguirei N.Robson	Maguire & Maguire 61707 (BM)	core Páramo	H	LT904602	LT904520	HG004732	—
H. majus (A.Gray) Britton	Rastetter s.n. (MA)	Am-As-Af	E	LT904603	—	KC709350	—
H. marahuacanum subsp. *marahuacanum* N.Robson	Nürk & Atchison 665 (ANDES, BM)	core Páramo	H	LT904604	LT904521	LT904661	LT904468
H. mexicanum L.	Nürk et al. 639 (ANDES, BM)	core Páramo	H	LT904605	LT904522	LT904662	LT904469
H. microsepalum (Torr. & A.Gray) A.Gray ex S.Watson	Crockett H-63 (UGA)	*Myriandra*	E	LT904606	—	LT904663	—
H. mutilum L.	Crockett 173 (UGA)	Am-As-Af	E	LT904607	LT904523	LT904664	—
H. myricariifolium Hieron.	Nürk & Atchison 526 (ANDES, BM)	core Páramo	H	LT904608	LT904524	HG004723	LT904470
H. myrtifolium Lam.	Crockett Hyp-7 (UGA)	*Myriandra*	E	LT904609	—	LT904665	—

Taxon (continued)	Specimen	Clade	Area	petD	trnL	ITS	AtG13040
H. nitidum subsp. *exile* Lam.	Crockett H-84 (UGA)	*Myriandra*	EFG	LT904610	—	LT904666	—
H. nudiflorum Michx.	Crockett H50ITS (UGA)	*Myriandra*	E	—	—	AY555888	—
H. parallelum N.Robson	Nürk et al. 620 (ANDES, BM)	core Páramo	H	LT904611	LT904525	LT904667	LT904471
H. perforatum L.	Nürk 483 (GAT)	outgroup	BC	LT904612	LT904526	LT904668	LT904472
H. phellos subsp. *phellos* Gleason	Nürk et al. 624 (ANDES, BM)	core Páramo	H	LT904613	LT904527	LT904669	LT904473
H. philonotis Schltdl. & Cham.	Förther 10060 (BM)	Páramo *affinis*	F	LT904614	—	HG004764	—
H. pimeleoides Planch. & Linden ex Triana & Planch.	Nürk & Atchison 559 (ANDES, BM)	core Páramo	H	LT904615	LT904528	LT904670	LT904474
H. polyanthemum Klotzsch ex Reichardt	Sobral s.n. (2007) (BM)	East S. America	JK	LT904616	—	HG004773	—
H. pratense Schltdl. & Cham.	Amith & Santiago 1102 (BM)	*Páramo affinis*	F	LT904617	LT904529	HG004765	—
H. prolificum L.	FB 1243 (in: Pilepic et al. 2011)	*Myriandra*	E	—	—	FJ694217	—
H. prostratum Cuatrec.	Nürk & Atchison 499 (ANDES, BM)	core Páramo	H	LT904618	LT904530	HG004685	LT904475
H. quitense R.Keller	Holm-Nielsen et al. 29216 (BM)	Páramo *affinis*	H	LT904619	LT904531	HG004736	—
H. rigidum subsp. *rigidum* A.St.-Hil.	Hatschbach 48170 (BM)	East S. America	JK	—	—	HG004775	—
H. ruscoides Cuatrec.	Nürk et al. 616 (ANDES, BM)	core Páramo	H	LT904620	LT904532	LT904671	LT904476
H. sabiniforme Trevir.	Nürk et al. 649 (ANDES, BM)	core Páramo	H	LT904621	LT904533	LT904672	LT904477
H. scioanum Chiov.	Gehrke 168 (Z)	Am-As-Af	A	LT904622	LT904534	LT904673	LT904478
H. selaginella N.Robson	Nürk et al. 644 (ANDES, BM)	core Páramo	H	LT904623	LT904535	LT904674	LT904479
H. silenoides Juss.	Hughes 3113 (HEID, B, MOL, Z)	Páramo *affinis*	HIK	LT904624	LT904536	HG004769	LT904480
H. sphaerocarpum Michx.	Crockett H-162 (UGA)	*Myriandra*	E	LT904625	LT904537	AY555878.2	—
H. sprucei N.Robson	Jørgensen et al. 2218 (BM)	core Páramo	H	LT904626	LT904538	HG004648	—
H. strictum Kunth	Nürk et al. 648 (ANDES, BM)	core Páramo	H	LT904627	LT904539	LT904675	LT904481
H. struthiolifolium Juss.	Smith 4126 (BM)	core Páramo	I	LT904628	LT904540	HG004756	—
H. suffruticosum W.P.Adams	Crockett 156 (UGA)	*Myriandra*	E	—	—	HE653637	—
H. tenuifolium Pursh	Crockett 126 (UGA)	*Myriandra*	E	LT904629	—	LT904676	LT904482
H. ternum A.St.-Hil.	Nicolack & Cordeiro 63 (BM)	East S. America	JK	LT904630	—	HG004776	—
H. terrae-firmae Sprague & Riley	Monro 741 (BM)	*Terrae-firmae*	F	LT904631	LT904541	HG004759	—
H. tetrapetalum Lam.	Crockett H44ITS (UGA)	*Myriandra*	E	—	—	AY555882.2	—
H. tetrastichum Cuatrec.	Nürk & Atchison 574 (ANDES, BM)	core Páramo	H	LT904632	LT904542	HG004666	LT904483
H. thesiifolium Kunth	Burger & Liesner 6439 (BM)	Páramo *affinis*	FH	LT904633	LT904543	HG004767	—
H. thuyoides Kunth	Nürk & Atchison 498 (ANDES, BM)	core Páramo	H	LT904634	LT904544	LT904677	LT904484
H. valleanum N.Robson	Nürk et al. 623 (ANDES, BM)	core Páramo	H	LT904635	LT904545	LT904678	LT904485
H. virginicum Raf.	Mitchel & Focht 8507 (GH)	*Triadenum*	E	—	LT904550	HE653667	—
H. walteri (J.F.Gmel.) Gleason	Crockett H-163 (UGA)	*Triadenum*	E	LT904639	—	LT904680	—
H. woodianum N.Robson	Nürk & Atchison 502 (ANDES, BM)	core Páramo	H	LT904636	LT904546	—	LT904486

2. Molecular marker:

Amplification of *pet*D, *trn*L, and ITS was done using primer combinations and PCR conditions tried and tested in the study system (Nürk *et al.*, 2013b; Nürk *et al.*, 2013a; Nürk *et al.*, 2015). Amplification of At1G13040 was done in 25 µl reactions using 1 U Taq DNA polymerase (QIAGEN, Hilden, Germany), 5 µl Q-solution (QIAGEN), 2.5 µl of the supplied buffer (10x), 100 µM of each dNTP, 5 pmol of each primer and approximately 20 ng of total DNA. PCR profiles consisted of an initial denaturation at 96°C for 1.5 min, followed by 35 cycles of 95°C for 30s, 55°C for 60s, 73°C for 90s and a final step at 72°C for 10 min.

The following primer combinations have been used for PCR amplification and sequencing:

(1) *pet*D (cp; including the *pet*B–*pet*D intergenic spacer, the *pet*D-5′-exon, and the *pet*D intron) using primer combination PI*pet*B1411F and PI*pet*D738R (Löhne & Borsch, 2005).

(2) *trn*L (cp; including the *trn*L^{UAA} intron) using primer combination *trn*L(F) ('c') and *trn*L(R) ('d') (Taberlet *et al.*, 1991).

(3) ITS (nt; rDNA internal transcribed spacer region including ITS-1, 5.8S rDNA, and ITS-2) using primer combination ITS-A(F) and ITS-B(R) (Blattner, 1999).

(4) the At1G13040 protein coding region (nt; a putative single-copy loci from the PPR gene family) using primer combination At1G13040-H145F (forward: 5'-TCC TTA GCG TCG ACT ACA ACC-3') and At1G13040-H908R (reverse: 5'-TCC AGC CGG TTA GCT TTA CA-3'). The single-copy nature was confirmed by sub-cloning of the PCR products in the pGEM-T Easy vector (Promega, Madison, WI, USA; two diploid *H. perforatum* with eight sequenced clones per individual, and selected species from the New World clade of *Hypericum* with four to ten sequenced clones per individual; results not shown). Single copy nature and homology to the At1G13040 gene was accessed by gene tree reconstructions and blastn similarity search in the NCBI web page (http://blast.ncbi.nlm.nih.gov). DNA sequencing was done by Eurofins MWG Operon (Ebersberg, Germany).

3. Age estimations: calibration

The following node ages have been constrained (fossils with uniform and secondary constrains with normal distributions):

(1) the root node age (*i.e.* the crown node of *Hypericum*) estimated to 25.9 Ma (19.6–33.3 95% HPD) (Nürk *et al.*, 2015) by a mean of 26.0 and a standard deviation (SD) of 3.0;

(2) the *Myriandra-perforatum* crown node age estimated to 23.7 Ma (18.1–30.4 95% HPD) (Nürk *et al.*, 2015) by a mean of 23.0 and 2.5 SD;

(3) the stem node of *Triadenum* (i.e. the New World *Hypericum* crown node) using the *Hypericum tertiaerum* Nikitin fossil seeds (Mai, 2000, 2001) from the Miocene of East Europe and Siberia with a minimum age of 5.3 Ma;

(4) the *Myriandra* crown node age estimated to 9.4 Ma (4.5–14.9 95% HPD) (Nürk *et al.*, 2015) by a mean of 9.8 and 3.0 SD;

(5) the stem node of 'Páramo *affinis* + core Páramo' using *Hypericum* pollen fossils (Van der Hammen *et al.*, 1973; Rutter *et al.*, 2012; Torres *et al.*, 2013) from the Upper Pliocene of high valleys of Colombia with a minimum age of 2.5 Ma (according to geomagnetic polarity the age of this pollen fossil has recently been dated near the Guass-Matuyama polarity reversal at 2.6 Ma (Rutter et al. 2012), and we made sensitivity analysis examining the impact of this updated age on our divergence time estimates. Because produced age estimates were identical, we kept the 'original' ages estimated under the 2.5 Ma constrain);

(6) the crown node age of the New World clade of *Triadenum* using seed fossils of *H. virginicum* (Miller & Calkin, 1992) from the Pleistocene of North America with a minimum age of .01 Ma.

4. Historical biogeography and biome shift analysis

Table S2.1. Areas used in the biogeographic estimation detailing the coordinates of the centroid used in the distance-dependent dispersal model (M_D, BayArea).

Area	Area code	Centroid of area	
		latitude	longitude
Africa	A	0.47193	29.94620
West Palaearctic	B	52.49636	13.42067
East Palaearctic	C	35.72722	139.73825
Asia tropical	D	-5.45514	142.40039
North America	E	23.67781	-101.80527
Central America	F	13.06736	-85.61072
Caribbean (West Indies)	G	18.37671	-71.55506
Northern Andes	H	4.75847	-75.36088
Central and Southern Andes	I	-15.26109	-73.36283
Eastern South America	J	-17.52867	-43.62986
South America temperate	K	-27.62008	-60.54290

Table S2.2. Biomes used in the biome-shift estimation detailing the 'coordinates' (obtained via multidimensional scaling of a distance matrix representing globally shared border between pairs of biomes) of the centroid used in the distance-dependent dispersal model (M_D, BayArea).

Biome		'latitude'	'longitude'
1	Tropical and Subtropical Moist Broadleaf Forests	100.084645	-2.252012
2	Tropical and Subtropical Dry Broadleaf Forests	48.314431	6.202495
3	Tropical and Subtropical Coniferous Forests	20.409976	-0.785878
4	Temperate Broadleaf and Mixed Forests	-66.135392	-4.690757
5	Temperate Coniferous Forests	-52.185679	-65.881461
6	Boreal Forests/Taiga	-52.163978	84.107604
7	Tropical and subtropical grasslands, savannas, and shrublands	59.465944	-6.552599
8	Temperate Grasslands, Savannas, and Shrublands	-40.173061	-14.351418
9	Flooded Grasslands and Savannas	4.485946	6.667280
10	Montane Grasslands and Shrublands	4.443463	-34.019600
11	Tundra	-5.692768	9.034944
12	Mediterranean Forests, Woodlands, and Scrub	-22.191629	-9.579940
13	Deserts and Xeric Shrublands	-0.718684	-51.489503
14	Mangroves	33.700708	33.355498

Ancestral area estimations: model comparison

Six biogeographic models have been compared on model fit (Table S3) and on estimation of ancestral areas (Figs S1) using the R package biogeobears (Matzke, 2012): (1) Dispersal-Extinction Cladogenesis Model (DEC), (2) DEC Model including the founder event (jump) parameter (DEC + j), (3) the ML implementation of the Dispersal-Vicariance Analysis

(DIVA-like), (4) DIVA-like with the founder parameter (DIVA-like + j), (5) the ML implementation of the BayArea model (BAYAREA-like), and the BayArea model with the founder parameter (BAYAREA-like + j). We evaluate the estimated model fit by comparing the second order sample size corrected Akaike Information Criterion (AICc) and Akaike weigths (AICc wt).

Table S3. Summary statistic of biogeographic model selection (biogeobears).

Model	Nº param.	lnL	AICc	ΔAICc	AICc wt
BAYAREA-like + j	3	-175.52569	357.3	0	$1.00e^{+00}$
DEC	2	-195.95118	396.0	38.7	$3.88e^{-09}$
DEC + j	3	-195.56545	397.4	40.1	$1.98e^{-09}$
DIVA-like + j	3	-200.02369	406.3	49.0	$2.29e^{-11}$
DIVA-like	2	-201.51068	407.1	49.9	$1.50e^{-11}$
BAYAREA-like	2	-206.38804	416.9	59.6	$1.14e^{-13}$

Nº param. = number of free model parameters (estimated parameters).
ΔAICc = difference of each model AICc to best model AICc
AICc wt = Akaike weight (relative likelihood of the model / sum of relative likelihoods of all models)
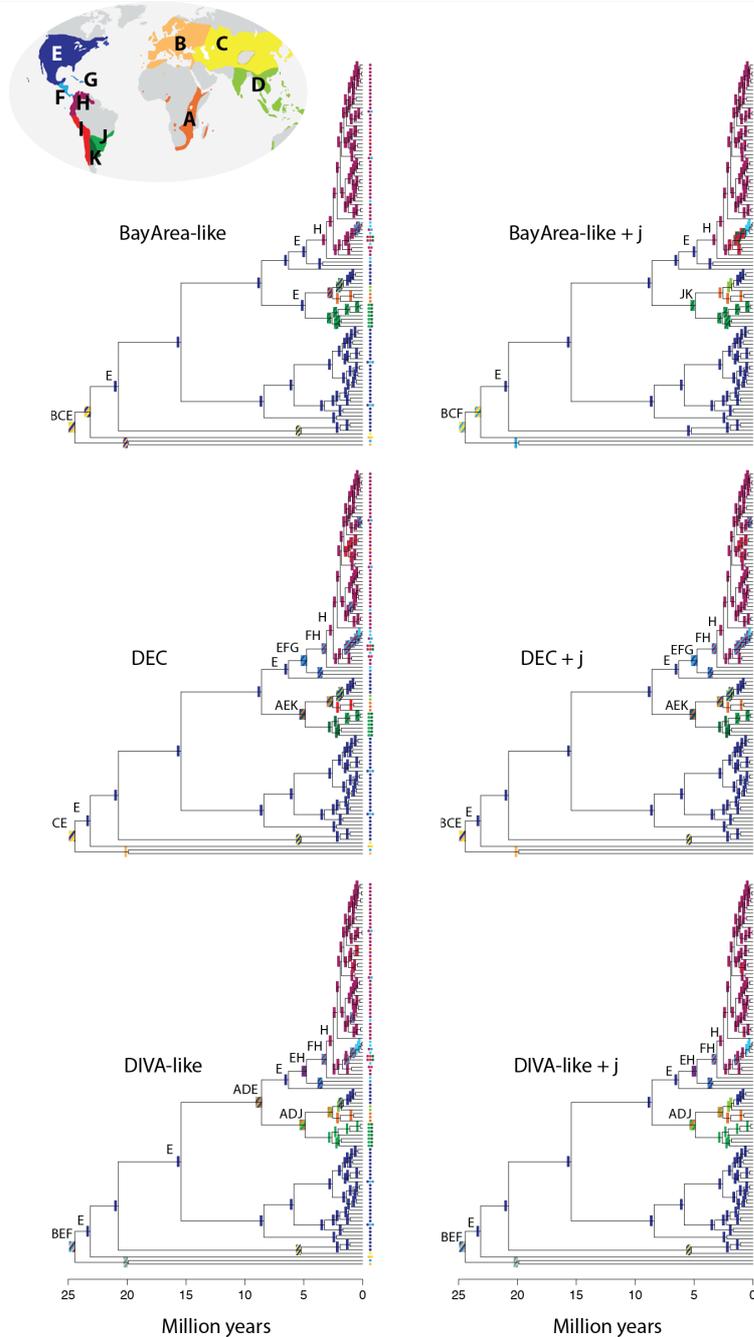
Fig. S1. Ancestral area estimations comparing six models (detailing most likely scenario per model; biogeobears).

Table S4. Summary statistics: node support, age estimation, historical biogeography and biome shifts to the mountain biome (MGS, biome 10; RAxML, BEAST, BayArea).

Clade (mrca)	Node support [pp | BS]	Crown ages [Ma]	Mountain biome [pp]	Biogeography Area	pp
Hypericum	—	24.4 (20.4–28.7)		**E Palearc**	**.36**
				Asia trop	.33
				W Palearc	.29
'New World' *Hypericum*	1 | 91	20.8 (17.0–24.7)	.18	**N Am**	**.39**
				E Palearc	.35
				Asia trop	.30
Triadenum	1 | 100	5.2 (2.6–8.9)	.06	**N Am**	**.64**
				E Palearc	.63
				Asia trop	.18
Myriandra – Andean radiation	1 | 100	15.4 (12.0–18.8)	.21	**N Am**	**.55**
				Asia trop	.26
				E Palearc	.23
Myriandra	1 | 100	8.4 (5.8–11.4)	.07	**N Am**	**.96**
				C Am	.20
				W Indies	.16
East South America – Andean radiation	1 | 100	8.6 (6.2–11.3)	.38	**N Am**	**.60**
				Asia trop	.26
				C Am	.23
East South America – America-Asia-Africa	1 | 100	4.9 (3.1–6.9)	.47	**eSA**	**.43**
				Af	.40
				SAtemp	.38
East South America	1 | 99	2.6 (1.5–4.0)	.04	**eSA**	**.98**
				tempSA	.97
				Af	.03
America-Asia-Africa	1 | 100	2.5 (15–3.8)	.97	**Asia trop**	**.69**
				Af	.68
				N Am	.24
Gentianoides – Andean radiation	1 | 100	6.3 (4.3–8.8)	.38	**N Am**	**.79**
				N Andes	.35
				C Am	.34
Drummondii – Andean radiation	.96 | 84	4.8 (3.3–6.7)	.44	**N Am**	**.73**
				N Andes	.54
				C Am	.40
Drummondii	.92 | 94	3.4 (1.6–5.4)	.22	**N Am**	**.79**
				W Indies	.46
				N Andes	.33
Andean radiation	1 | 85	3.1 (2.0–4.3)	.73	**N Andes**	**.87**
				C Am	.49
				N Am	.15
Páramo *affinis* + core Páramo	.86 | 64	2.5 (1.8–3.4)	.99	**N Andes**	**1.00**
				C Am	.49
				C+S Andes	.11
Páramo *affinis*	.98 | 57	2.1 (1.3–2.9)	.99	**N Andes**	**1.00**
				C+S Andes	.26
				C Am	.26
core Páramo	.99 | 67	1.9 (1.3–2.5)	1.00	**N Andes**	**1.00**
				C Am	.09
				C+S Andes	.05

5. Environmental space and niche similarity tests

Climate and elevation data was extracted for the entire *Hypericum* occurrence dataset and the New World spatial points dataset from the WorldClim climate layers version 1.3 (Hijmans *et al.*, 2005) with a spatial resolution of 30-s. We extracted the 19 Bioclimatic variables and elevation above sea level. To account for the limiting environmental factor 'minimum temperatures during the growing season (vegetation period; T_{minVeg}) we defined four phenological zones arbitrarily delimited by latitude (Table S5) and extracted the monthly minimum temperature per occurrence/spatial point with a spatial resolution of 30-s (Hijmans *et al.*, 2005) using raster 2.3-33 in R (Hijmans, 2015). The minimum value per occurrence/spatial point was calculated based on the definition of the phenological zone to obtain T_{minVeg}. To test for the sensitivity to the delimitation of the phenological zone we create three variables with sequentially prolonged 'zone' definitions (*NB*, we regard the beginning of the vegetation period as limiting since freezing damage during bud-burst is most problematic for the plant, hence, we vary the beginning of the vegetation period; Table S5).

Table S5. Definition of phenologic zones used to understand adaptation to minimum temperatures during vegetation period.

Variable	Zone	Maximum latitude	Minimum latitude	Duration (month)	
				Start	End
T_{minVeg}	1		> 40.00	5	9
	2	≤ 40.00	> 23.437	4	9
	3	≤ 23.437	≥ -23.437	1	12
	4	< -23.437		10	2
$T_{minVeg2}$	1		> 40.00	4	9
	2	≤ 40.00	> 23.437	3	9
	3	≤ 23.437	≥ -23.437	1	12
	4	< -23.437		9	2
$T_{minVeg3}$	1		> 40.00	3	9
	2	≤ 40.00	> 23.437	2	9
	3	≤ 23.437	≥ -23.437	1	12
	4	< -23.437		8	2

Table S6. Definition of entities (species, regions) used to calculate pairwise Schoener's *D* (ecospat).

Entity (region)	Abbreviation	Maximum latitude	Minimum latitude	Maximum altitude	Minimum altitude
North America temperate lowlands	*NA TmpLow*	≤ 59.996	> 23.437	≤ 1000	≥ 0
North America temperate montane	*NA TmpMt*	≤ 59.996	> 23.437	≤ 5000	≥ 1001
South America tropic lowlands	*SA TrpLow*	≤ 23.437	≥ -23.437	≤ 1000	≥ 0
S America tropic montane north of Páramo	*SA TrpMt-n*	≤ 23.430	> 11.000	≤ 3000	≥ 1001
S America tropic montane range of Páramo	*SA TrpMt-P*	≤ 11.000	≥ -8.000	≤ 3000	≥ 1001
S America tropic montane south of Páramo	*SA TrpMt-s*	< -8.000	≥ -23.437	≤ 3000	≥ 1001
S America tropic alpine – Páramo	*SA TrpAlp-Páramo*	≤ 11.000	≥ -8.000	≤ 5000	≥ 3001
S America tropic alpine south of Páramo	*SA TrpAlp-s*	< -8.000	≥ -23.437	≤ 5000	≥ 3001
South America temperate lowlands	*SA TmpLow*	< -23.437	≥ -39.979	≤ 1000	≥ 0
South America temperate montane	*SA TmpMt*	< -23.437	≥ -39.979	≤ 5000	≥ 1001

Entity (species)		Clade			
North American species	*NA spec*	*Triadenum + Myriandra + Gentianoides + Drummondii*			
Andean radiation species	*Andean spec*	Andean radiation			
East South American species	*eSA spec*	*Trigynobrathys* s.str. – East South American			

Table S7. Definition of sequentially enlarged backgrounds (ranges) used in the niche similarity test (ecospat).

Background	Seq.	Maximum latitude	Minimum latitude	Minimum altitude	Maximum altitude
Range N American species	1	≤ 52.099	≥ 14.230	≥ -2	≤ 2303
	2	≤ 53.099	≥ 15.230	≥ -12	≤ 2403
	3	≤ 54.099	≥ 16.230	≥ -22	≤ 2503
	4	≤ 55.099	≥ 17.230	≥ -32	≤ 2603
	5	≤ 56.099	≥ 18.230	≥ -42	≤ 2703
Range Andean species	1	≤ 21.480	≥ -26.710	≥ 10	≤ 5096
	2	≤ 22.480	≥ -27.710	≥ 0	≤ 5196
	3	≤ 23.480	≥ -28.710	≥ -10	≤ 5296
	4	≤ 24.480	≥ -29.710	≥ -20	≤ 5396
	5	≤ 25.480	≥ -30.710	≥ -30	≤ 5496
Range East South American species	1	≤ -14.500	≥ -34.370	≥ 11	≤ 2194
	2	≤ -13.500	≥ -35.370	≥ 1	≤ 2294
	3	≤ -12.500	≥ -36.370	≥ -9	≤ 2394
	4	≤ -11.500	≥ -37.370	≥ -19	≤ 2494
	5	≤ -10.500	≥ -38.370	≥ -29	≤ 2594

Table S8. Climate similarity pairwise between tropical alpine Páramo and different potential source regions given as Schoener's *D* (mean and sd).

Parameter	Páramo & NA TmpLow Mean	sd	Páramo & NA TmpMt Mean	sd	Páramo & SA TrpLow Mean	sd	Páramo & SA TrpMt-n Mean	sd	Páramo & SA TrpMt-P Mean	sd	Páramo & SA TrpMt-s Mean	sd	Páramo & SA TrpAlp-s Mean	sd	Páramo & SA TmpLow Mean	sd	Páramo & SA TmpMt Mean	sd
Axis 1	.490	.085	.033	.010	.190	.087	.204	.008	.584	.032	.025	.004	.087	.013	.531	.069	.045	.005
Axis 2	.333	.096	.207	.056	.285	.049	.096	.027	.571	.032	.027	.006	.033	.005	.470	.030	.067	.010
Axis 3	.312	.065	.129	.070	.412	.117	.259	.033	.362	.044	.084	.036	.356	.055	.317	.051	.300	.071
Ax mean	**.378**		**.123**		**.296**		**.187**		**.506**		**.045**		**.159**		**.440**		**.137**	
Altitude	0	0	.316	.052	0	0	.074	.013	.186	.009	.189	.008	.721	.030	0	0	.341	.015
T_{mean}	.015	.004	.413	.124	0	0	.182	.024	.295	.023	.270	.023	.791	.030	.050	.013	.507	.033
$T_{rangeDay}$	.370	.113	.203	.030	.412	.081	.021	.003	.491	.087	.218	.036	.136	.012	.490	.052	.278	.049
T_{iso}	0	0	.004	.003	.492	.051	.040	.004	.744	.053	.468	.050	.194	.024	0	0	.046	.009
T_{seas}	0	0	0	0	.278	.013	.013	.001	.812	.021	.208	.010	.011	.002	0	0	0	0
T_{max}	.283	.047	.224	.071	.003	.002	.649	.023	.369	.023	.524	.031	.501	.017	.115	.019	.396	.031
T_{min}	.348	.063	.392	.079	0	0	.183	.053	.288	.035	.235	.031	.598	.037	.003	.002	.510	.058
T_{minVeg}	.142	.050	.295	.018	.002	.001	.725	.016	.244	.020	.488	.024	.498	.022	.370	.072	.192	.015
T_{range}	.182	.044	.016	.010	.523	.034	.092	.005	.790	.024	.521	.030	.011	.002	.166	.021	.163	.013
T_{wet}	.305	.024	.119	.015	0	.001	.116	.019	.222	.017	.154	.020	.740	.014	.157	.041	.389	.030
T_{dry}	.081	.014	.412	.020	0	0	.225	.021	.210	.023	.302	.026	.773	.025	.162	.069	.275	.013
T_{warm}	.258	.037	.366	.068	0	0	.096	.024	.241	.019	.162	.020	.749	.022	.005	.003	.604	.021
T_{cold}	.066	.044	.320	.020	0	.001	.257	.017	.159	.015	.263	.017	.740	.023	.282	.049	.175	.011
T mean	**.171**		**.230**		**.143**		**.216**		**.405**		**.318**		**.478**		**.150**		**.295**	
P_{ann}	.443	.079	.362	.033	.281	.076	.237	.027	.293	.050	.272	.051	.310	.017	.566	.103	.309	.022
P_{max}	.209	.100	.214	.075	.360	.088	.308	.039	.423	.073	.338	.085	.465	.017	.478	.087	.303	.015
P_{min}	.693	.154	.438	.052	.261	.096	.308	.114	.380	.060	.390	.086	.121	.008	.661	.087	.342	.024
P_{seas}	.176	.034	.136	.015	.229	.073	.038	.003	.612	.038	.055	.011	.013	.002	.472	.022	.057	.017
P_{wet}	.241	.066	.288	.044	.344	.090	.297	.028	.336	.042	.290	.037	.438	.019	.472	.066	.294	.015
P_{dry}	.710	.113	.436	.039	.264	.091	.316	.028	.407	.070	.398	.081	.119	.011	.673	.152	.349	.028
P_{warm}	.617	.158	.278	.054	.336	.110	.416	.055	.557	.056	.379	.191	.378	.015	.531	.102	.240	.019
P_{cold}	.436	.071	.327	.033	.390	.117	.213	.025	.319	.054	.366	.066	.136	.007	.642	.134	.594	.039
P mean	**.441**		**.310**		**.308**		**.267**		**.416**		**.311**		**.248**		**.562**		**.311**	

Table S9.1. Results of the niche similarity test under sequentially enlarged backgrounds (ranges).

Parameter	North American *vs.* Andean radiation											
	Niche overlap	Niche expansion	Niche similarity test *P* {divergence}					Niche similarity test *P* {conservatism}				
			Range 1	Range 2	Range 3	Range 4	Range 5	Range 1	Range 2	Range 3	Range 4	Range 5
Axis 1	.618	.029	1	1	1	1	1	.422	.476	.478	.512	.516
Axis 2	.661	.069	1	1	1	1	1	**.006**	**.003**	**.003**	.168	.057
Axis 3	.066	.177	**.006**	**.012**	**.003**	**.009**	**.003**	1	.997	1	.998	1
Altitude	.041	.878	1	.760	.672	.900	1	1	1	1	1	1
T_{mean}	.208	.012	1	1	1	1	1	1	1	1	1	1
$T_{rangeDay}$	.470	.033	1	1	1	1	1	.969	1	1	1	1
T_{iso}	.375	.288	1	1	1	1	1	1	1	1	1	1
T_{seas}	.245	0	1	1	1	1	1	.154	1	1	1	1
T_{max}	.012	.734	.110	.066	**.044**	**.023**	.176	1	1	1	1	1
T_{min}	.540	.001	1	1	1	1	1	1	1	1	1	1
T_{minVeg}	.247	.042	1	1	1	1	1	1	1	1	1	1
$T_{minVeg2}$	.398	.009	1	1	1	1	1	1	1	1	1	1
$T_{minVeg3}$	.567	.004	1	1	1	1	1	1	1	1	1	1
T_{range}	.250	.289	.336	.672	.672	.588	.903	1	1	1	1	1
T_{wet}	.149	0	1	1	1	1	1	.720	.644	.368	**.023**	1
T_{dry}	.376	0	1	1	1	1	1	1	1	1	1	1
T_{warm}	.022	.728	**.046**	**.046**	**.023**	**.023**	**.023**	1	1	1	1	1
T_{cold}	.534	0	1	1	1	1	1	1	1	1	1	1
P_{ann}	.399	.088	1	1	1	1	1	1	1	1	1	1
P_{max}	.501	.090	1	1	1	1	1	1	1	1	1	1
P_{min}	.204	.091	1	1	1	1	1	1	1	1	1	1
P_{seas}	.156	.042	1	1	1	1	1	.023	1	1	1	1
P_{wet}	.504	.080	1	1	1	1	1	1	1	1	1	1
P_{dry}	.196	.068	1	1	1	1	1	1	1	1	1	1
P_{warm}	.440	.013	1	1	1	1	1	1	1	1	1	1
P_{cold}	.613	.117	1	1	1	1	1	.651	1	1	1	1

p-values adjusted with Holm's correction (controlling for family-wise error rate; Holm 1979)

Table S9.2. Results of the niche similarity test under sequentially enlarged backgrounds (ranges).

Parameter	North American *vs.* East South American											
	Niche overlap	Niche expansion	Niche similarity test *P* {divergence}					Niche similarity test *P* {conservatism}				
			Range 1	Range 2	Range 3	Range 4	Range 5	Range 1	Range 2	Range 3	Range 4	Range 5
Axis 1	.628	0	1	1	1	1	1	**.046**	.271	.234	.214	.198
Axis 2	.226	.086	1	1	1	1	1	**.003**	**.003**	**.003**	**.006**	**.006**
Axis 3	.693	.004	1	1	1	1	1	**.046**	.080	.112	.060	.090
Altitude	.324	.071	.374	.462	.616	.736	1	1	1	1	1	1
T_{mean}	.627	0	1	1	1	1	1	1	.702	1	.975	.324
$T_{rangeDay}$	.613	.012	1	1	1	1	1	1	.352	.357	1	1
T_{iso}	.387	0	1	1	1	1	1	.450	.221	1	1	1
T_{seas}	.304	0	.840	1	1	1	1	1	1	1	1	1
T_{max}	.312	.008	1	1	1	1	.483	1	1	1	1	1
T_{min}	.555	0	1	1	1	1	1	1	**.040**	1	.672	.266
T_{minVeg}	.451	.001	1	1	1	1	1	**.046**	**.023**	.126	.120	.324
$T_{minVeg2}$	.768	0	1	1	1	1	1	1	1	1	1	1
$T_{minVeg3}$	.613	0	1	1	1	1	1	1	1	1	1	1
T_{range}	.374	0	.840	1	1	1	1	1	1	1	1	1
T_{wet}	.143	0	.253	.184	.092	.748	1	1	1	1	1	1
T_{dry}	.417	0	1	1	1	1	1	1	1	1	1	1
T_{warm}	.359	0	.374	.462	.616	.882	.748	1	1	1	1	1
T_{cold}	.489	0	1	1	1	1	1	1	1	1	1	1
P_{ann}	.425	.027	1	1	1	1	1	1	1	1	1	1
P_{max}	.720	0	1	1	1	1	1	.544	.434	.624	.476	.525
P_{min}	.344	.077	1	1	1	1	1	**.046**	**.023**	**.046**	**.046**	**.023**
P_{seas}	.478	.052	1	1	1	1	1	**.046**	**.023**	.126	.063	.066
P_{wet}	.676	0	1	1	1	1	1	1	.960	1	.975	.924
P_{dry}	.627	.067	1	1	1	1	1	.066	**.040**	.088	**.046**	.084
P_{warm}	.457	0	1	1	1	1	1	.152	.126	.171	.190	.084
P_{cold}	.405	.013	1	1	1	1	1	.752	.405	.306	.360	.324

p-values adjusted with Holm's correction (controlling for family-wise error rate; Holm 1979)

6. Niche shift analysis
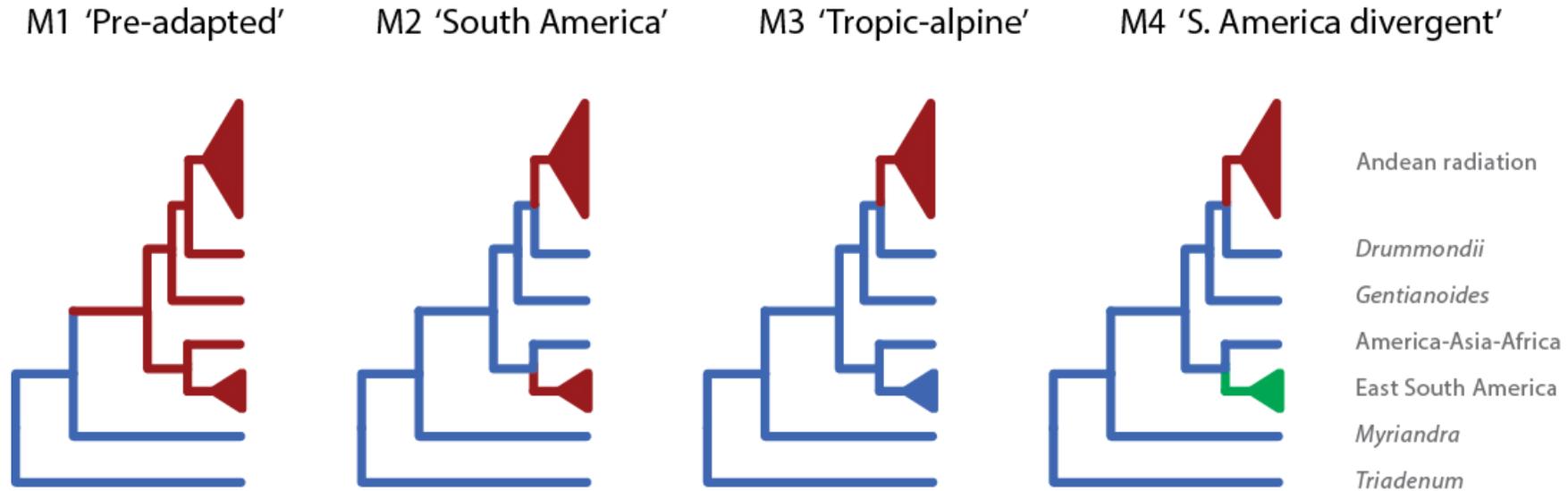
Figure S2. Regime models: evolutionary scenarios used to test on niche shifts prior to ('pre-adaptation') or with establishment of tropical alpine lineages (*in situ* adaptation).

We consider a model as supported with evidence if BF >2 compared to other models (Kass & Raftery, 1995). We only reject pre-adaptation (M1 model) if another model (M2-M4) is supported with BF > 2 over M1. Similarly, we only accept *in situ* adaptation in the tropical alpine environments (M3/M4) if M3 or M4 is favored over M1 or M2 with BF > 2. Example: we interpret BF for M4 over M1 >2, and BF for M4 over M2 ≤2, and BF for M2 over M1 <2 as no supported evidence for *in situ* adaptation, and conclude on pre-adaption.

Table S10.1. Phylogenetic signal (Blomberg's K), results of model fit analysis (*fitContinuous* in geiger) and of niche shift analysis (bayou)

Analysis Parameter	*Hypericum* on NW-PCA [median]			*Hypericum* on NW-PCA [qts]			Altitude	
	Axis1	Axis2	Axis3	Axis1	Axis2	Axis3	median	.95-qts
Phylogenetic signal	.108**	.089*	.448**	.097**	.092**	.352**	.922*	.987*
Model fit (estimating SE)								
lnL{WN}	-97.7	-134.2	-164.9	-101.8	-146.5	-158.2	-907.1	-916.0
lnL{BM}	-103.2	-152.4	-109.1	-101.8	-135.8	-92.9	-824.8	-829.7
lnL{OU}	-93.5	-117.5	-84.5	-97.6	-132.3	-91.7	-817.6	-823.6
AICc{WN}	201.7	274.6	336.0	209.8	299.3	322.7	1820.5	1838.3
AICc{BM}	212.7	311.1	224.5	209.8	277.8	192.0	1655.8	1665.6
AICc{OU}	195.3	243.5	177.5	203.6	272.9	191.9	1643.6	1655.6
ΔAICc{WN}	6.3	31.2	158.5	6.2	26.3	130.8	176.9	182.7
ΔAICc{BM}	17.4	67.6	47.0	6.2	4.9	2.1	12.1	10.0
ΔAICc{OU}	0	0	0	0	0	0	0	0
Niche shift								
Marginal lnL{Pre-adapted M1}	-94.8	-134.8	-104.7	-101.7	**-143.4**	-108.5	-843.1	-850.4
Marginal lnL{South America M2}	**-75.1**	-135.5	-103.3	**-97.0**	-145.5	-106.5	-842.9	**-850.2**
Marginal lnL{Tropical alpine M3}	-82.9	**-134.4**	**-94.5**	-98.7	-145.5	**-101.0**	**-842.2**	-850.6
Marginal lnL{S. America divergent M4}	-76.6	-135.8	-96.4	-98.5	-146.9	-102.0	-846.1	-853.9
BF {favoring M2 over M1}	39.5	-1.2	2.8	9.5	-4.3	4.0	.5	.4
BF {favoring M3 over M1}	23.9	.9	20.3	6.0	-4.2	15.1	1.8	-.6
BF {favoring M3 over M2}	-15.6	2.1	17.5	-3.5	.1	11.0	1.3	-1.0
BF {favoring M4 over M1}	36.5	-1.8	16.4	6.5	-7.0	13.0	-6.0	-7.0
BF {favoring M4 over M2}	-3.1	-.6	13.7	-3.0	-2.7	9.0	-6.5	-7.4
BF {favoring M4 over M3}	12.6	-2.7	-3.9	.5	-2.8	-2.1	-7.8	-6.4
Best Model (bold = significant)	**M2**	M3	**M3**	**M2**	**M1**	**M3**	M3	M2
Interpretation	SA	Pre	Trp-alp	SA	Pre	Trp-alp	Pre	Pre

Significance level: *p ≤ .05, **p ≤ .01, *p*-values adjusted with Holm's correction (controlling for family-wise error rate; Holm 1979). qts, quantile, i.e. the peripheral preferences.
Pre, pre-adaptation; SA, common niche optimum due to dispersal to South America (SA effect); Trp-alp, niche shift with dispersal and establishment in the tropical alpine environment.

Table S10.2. Phylogenetic signal (Blomberg's K), results of model fit analysis (*fitContinuous* in geiger) and of niche shift analysis (bayou)

Analysis Parameter	T_{mean} median	.5-qts	$T_{rangeDay}$ median	.95-qts	T_{iso} median	.95-qts	T_{seas} median	.95-qts	T_{max} median	.95-qts	T_{min} median	.5-qts
Phylogenetic signal	.161*	.196*	.076*	.094*	1.700*	.977*	1.571*	1.321*	.724*	.378*	.192*	.202*
Model fit (estimating SE)												
lnL{WN}	-550.3	-561.9	-453.2	-465.4	-458.4	-454.4	-168.3	-165.9	-600.7	-588.7	-564.4	-552.4
lnL{BM}	-530.4	-531.3	-476.6	-477.9	-352.4	-377.8	-63.9	-69.6	-525.7	-543.5	-556.7	-552.3
lnL{OU}	-517.9	-522.8	-446.8	-452.8	-352.0	-374.6	-60.5	-65.5	-518.5	-532.2	-546.6	-542.8
AICc{WN}	1106.8	1130.0	912.7	937.0	923.0	915.1	340.7	335.9	1207.7	1183.6	1135.1	1111.0
AICc{BM}	1067.0	1068.8	959.4	962.1	712.5	761.8	131.9	143.4	1057.6	1093.3	1119.5	1110.8
AICc{OU}	1044.2	1054.0	902.1	914.1	711.1	757.6	127.3	137.2	1045.5	1072.7	1101.6	1094.0
ΔAICc{WN}	62.6	76.0	10.6	22.9	211.9	157.4	213.4	198.8	162.2	110.9	33.4	17.0
ΔAICc{BM}	22.8	14.8	57.4	48.0	1.4	4.1	4.6	6.2	12.1	20.6	17.9	16.9
ΔAICc{OU}	0	0	0	0	0	0	0	0	0	0	0	0
Niche shift												
Marginal lnL{Pre-adapted M1}	-531.1	-536.7	-453.8	-465.0	-360.8	-383.1	-67.2	-72.0	-523.5	-534.6	-558.7	-554.7
Marginal lnL{South America M2}	**-528.6**	-535.7	-444.6	-459.2	-359.5	-382.2	-63.4	-68.4	-530.9	-540.6	-556.8	-554.0
Marginal lnL{Tropical alpine M3}	-531.4	-535.1	-445.0	**-458.7**	**-358.5**	**-381.7**	-59.8	-65.3	-535.6	-550.4	-560.2	-554.9
Marginal lnL{S. Am. divergent M4}	-529.4	**-533.6**	**-444.1**	-459.2	-358.4	-382.3	**-59.1**	**-65.0**	-541.4	-557.9	-557.5	-551.8
BF {favoring M2 over M1}	5.1	2.0	18.3	11.6	2.5	1.9	7.5	7.3	-14.8	-11.9	3.9	1.3
BF {favoring M3 over M1}	-.5	3.3	17.6	12.6	4.6	2.7	14.6	13.5	-24.1	-31.4	-3.0	-.5
BF {favoring M3 over M2}	-5.5	1.2	-.7	1.0	2.1	.8	7.1	6.1	-9.3	-19.5	-6.9	-1.7
BF {favoring M4 over M1}	3.5	6.2	19.3	11.6	4.8	1.6	16.1	14.0	-35.7	-46.6	2.5	5.8
BF {favoring M4 over M2}	-1.5	4.1	1.1	0	2.3	-.2	8.5	6.7	-20.9	-34.7	-1.4	4.5
BF {favoring M4 over M3}	4.0	2.9	1.8	-1.0	.2	-1.1	1.4	.6	-11.6	-15.1	5.5	6.2
Best Model (bold = significant)	**M2**	**M4**	M4	M3	**M3**	M3	**M4**	**M4**	**M1**	**M1**	**M2**	**M4**
Interpretation	SA	Trp-alp	SA	SA	Trp-alp	Pre	Trp-alp	Trp-alp	Pre	Pre	SA	Trp-alp

Significance level: *p ≤ .05, **p ≤ .01, *p*-values adjusted with Holm's correction (controlling for family-wise error rate; Holm 1979). qts, quantile, i.e. the peripheral preferences.
Pre, pre-adaptation; SA, common niche optimum due to dispersal to South America (SA effect); Trp-alp, niche shift with dispersal and establishment in the tropical alpine environment.

Table S10.3. Phylogenetic signal (Blomberg's K), results of model fit analysis (*fitContinuous* in geiger) and of niche shift analysis (bayou)

Analysis Parameter	T_{minVeg} median	.5-qts	$T_{minVeg2}$ median	.5-qts	$T_{minVeg3}$ median	.5-qts	T_{range} median	.95-qts	T_{wet} median	.95-qts	T_{dry} median	.95-qts
Phylogenetic signal	.106*	.136*	.085*	.104*	.143*	.174*	.921*	.957*	.195*	.227*	.109*	.114*
Model fit (estimating SE)												
lnL{WN}	-538.9	-550.2	-528.9	-536.2	-545.1	-555.3	-625.1	-637.4	-583.2	-581.1	-567.3	-553.3
lnL{BM}	-543.1	-541.4	-544.8	-541.7	-549.2	-548.9	-550.2	-559.2	-556.8	-558.2	-569.4	-553.7
lnL{OU}	-520.3	-523.7	-523.9	-526.1	-536.0	-540.0	-545.4	-555.7	-546.6	-544.5	-555.8	-534.1
AICc{WN}	1084.1	1106.6	1063.9	1078.7	1096.5	1116.8	1256.5	1281.0	1172.6	1168.5	1140.8	1112.9
AICc{BM}	1092.4	1089.0	1095.9	1089.6	1104.6	1103.9	1106.6	1124.6	1119.7	1122.7	1145.1	1113.7
AICc{OU}	1049.1	1055.9	1056.2	1060.7	1080.3	1088.5	1099.2	1119.8	1101.5	1097.4	1120.1	1076.6
ΔAICc{WN}	35.0	50.7	7.7	18.1	16.2	28.4	157.2	161.1	71.1	71.1	20.7	36.3
ΔAICc{BM}	43.3	33.1	39.7	28.9	24.3	15.5	7.4	4.8	18.2	25.3	25.0	37.1
ΔAICc{OU}	0	0	0	0	0	0	0	0	0	0	0	0
Niche shift												
Marginal lnL{Pre-adapted M1}	-534.7	-538.1	-538.2	-540.2	-548.0	-552.1	**-557.6**	-574.0	-560.2	**-555.0**	**-568.3**	-546.9
Marginal lnL{South America M2}	-535.0	-538.1	-537.0	-539.3	**-544.7**	**-551.7**	-562.8	**-573.7**	-560.1	-555.3	-570.5	**-540.7**
Marginal lnL{Tropical alpine M3}	**-530.8**	**-534.8**	-538.3	-540.4	-549.0	-553.6	-565.1	-574.6	**-559.0**	-562.0	-569.9	-543.5
Marginal lnL{S. Am. divergent M4}	-531.5	-537.0	**-536.8**	**-539.0**	-546.8	-552.6	-564.1	-574.7	-561.7	-561.5	-568.9	-542.0
BF {favoring M2 over M1}	-.6	-.1	2.4	1.9	6.6	1.0	-10.5	.6	.1	-.5	-4.5	12.5
BF {favoring M3 over M1}	7.8	6.5	-.2	-.3	-2.0	-2.9	-15.2	-1.2	2.4	-14.0	-3.3	6.8
BF {favoring M3 over M2}	8.4	6.6	-2.6	-2.2	-8.6	-3.8	-4.7	-1.7	2.2	-13.5	1.2	-5.7
BF {favoring M4 over M1}	6.5	2.2	2.9	2.4	2.4	-1.0	-13.1	-1.4	-3.0	-13.0	-1.3	9.9
BF {favoring M4 over M2}	7.0	2.3	.5	.5	-4.2	-1.9	-2.6	-1.9	-3.1	-12.5	3.2	-2.6
BF {favoring M4 over M3}	-1.4	-4.3	3.1	2.7	4.5	1.9	2.0	-.2	-5.4	1.0	2.0	3.1
Best Model (bold = significant)	**M3**	**M3**	M4	M4	**M2**	M2	**M1**	M2	**M3**	M1	M1	**M2**
Interpretation	Trp-alp	Trp-alp	SA	Pre	SA	Pre	Pre	Pre	Trp-alp	Pre	Pre	SA

Significance level: *p ≤ .05, **p ≤ .01, *p*-values adjusted with Holm's correction (controlling for family-wise error rate; Holm 1979). qts, quantile, i.e. the peripheral preferences.
Pre, pre-adaptation; SA, common niche optimum due to dispersal to South America (SA effect); Trp-alp, niche shift with dispersal and establishment in the tropical alpine environment.

Table S10.4. Phylogenetic signal (Blomberg's K), results of model fit analysis (*fitContinuous* in geiger) and of niche shift analysis (bayou)

Analysis Parameter	T_{warm} median	.95-qts	T_{cold} median	.5-qts	P_{min} median	.5-qts	P_{seas} median	.95-qts
Phylogenetic signal	.645*	.339*	.217*	.264*	.182*	.113*	.095*	.108*
Model fit (estimating SE)								
lnL{WN}	-592.0	-581.7	-562.2	-579.1	-484.8	-474.7	-450.1	-465.1
lnL{BM}	-521.9	-542.1	-545.8	-552.8	-473.5	-479.7	-466.8	-472.2
lnL{OU}	-514.1	-529.6	-538.7	-548.5	-459.7	-463.3	-442.4	-455.2
AICc{WN}	1190.2	1169.7	1130.7	1164.3	975.9	955.7	906.5	936.4
AICc{BM}	1050.1	1090.4	1097.9	1111.8	953.3	965.6	939.8	950.6
AICc{OU}	1036.6	1067.7	1085.7	1105.3	927.8	935.0	893.2	918.8
ΔAICc{WN}	153.6	102.0	45.0	59.0	48.1	20.6	13.3	17.6
ΔAICc{BM}	13.5	22.7	12.2	6.5	25.5	30.5	46.5	31.8
ΔAICc{OU}	0	0	0	0	0	0	0	0
Niche shift								
Marginal lnL{Pre-adapted M1}	**-523.8**	-535.0	-551.3	-561.2	-470.5	**-471.1**	-448.7	**-463.4**
Marginal lnL{South America M2}	-529.3	-539.1	**-551.0**	**-560.9**	-471.9	-475.6	-450.4	-466.6
Marginal lnL{Tropical alpine M3}	-531.9	**-533.2**	-551.0	-561.6	**-467.3**	-472.9	**-445.0**	-466.4
Marginal lnL{S. America divergent M4}	-531.2	-546.0	-551.0	-561.6	-467.5	-474.3	-445.8	-467.2
BF {favoring M2 over M1}	-10.9	-8.1	.7	.6	-2.8	-9.1	-3.3	-6.4
BF {favoring M3 over M1}	-16.1	3.6	.6	-.8	6.4	-3.7	7.6	-6.1
BF {favoring M3 over M2}	-5.2	11.7	-.1	-1.4	9.2	5.4	10.9	.4
BF {favoring M4 over M1}	-14.8	-21.9	.6	-.8	6.0	-6.5	5.8	-7.6
BF {favoring M4 over M2}	-3.8	-13.8	-.1	-1.4	8.8	2.6	9.2	-1.1
BF {favoring M4 over M3}	1.3	-25.5	0	0	-.4	-2.7	-1.8	-1.5
Best Model (bold = significant)	M1	**M3**	M2	M2	**M3**	**M1**	**M3**	**M1**
Interpretation	Pre	Trp-alp	Pre	Pre	Trp-alp	Pre	Trp-alp	Pre

Significance level: *p ≤ .05, **p ≤ .01, *p*-values adjusted with Holm's correction (controlling for family-wise error rate; Holm 1979). qts, quantile, i.e. the peripheral preferences.
Pre, pre-adaptation; SA, common niche optimum due to dispersal to South America (SA effect); Trp-alp, niche shift with dispersal and establishment in the tropical alpine environment.

7. References (SI)

Blattner, F.R. (1999) Direct amplification of the entire ITS region from poorly preserved plant material using recombinant PCR. *BioTechniques*, 27, 1180–1186.

Hijmans, R.J. (2015) *raster: Geographic data analysis and modeling*. [R package]

Hijmans, R.J., Cameron, S.E., Parra, J.L., Jones, P.G. & Jarvis, A. (2005) Very high resolution interpolated climate surfaces for global land areas. *International Journal of Climatology*, 25, 1965–1978.

Kass, R.E. & Raftery, A.E. (1995) Bayes Factors. *Journal of the American Statistical Association*, 90, 773–795.

Löhne, C. & Borsch, T. (2005) Molecular evolution and phylogenetic utility of the *pet*D group II intron: a case study in basal angiosperms. *Molecular Biology and Evolution*, 22, 317–332.

Mai, D.H. (2000) Die untermiozänen Floren aus der Spremberger Folger und dem II Flözhorizont der Lausitz. Teil III. Dialypetalae und Sympetalae. *Palaeontographica Abt B*, 253, 1–106.

Mai, D.H. (2001) Die mittelmiozänen und obermiozänen Floren aus der Meuroer und Raunoer Folge in der Lausitz. III. Fundstellen und Palaeobiologie. *Palaeontographica Abt B*, 258, 1–85.

Matzke, N.J. (2012) Founder-event speciation in BioGeoBEARS package dramatically improves likelihoods and alters parameter inference in Dispersal-Extinction-Cladogenesis (DEC) analyses. *Frontiers of Biogeography*, 4, 210.

Miller, N.J. & Calkin, P.E. (1992) Paleoecological interpretation and age of an interstadial lake bed in western New York. *Quaternary Research*, 37, 75–88.

Nürk, N.M., Scheriau, C. & Madriñán, S. (2013a) Explosive radiation in high Andean *Hypericum*– Rates of diversification among New World lineages. *Frontiers in Genetics*, 4, 1–14.

Nürk, N.M., Madriñán, S., Carine, M.A., Chase, M.W. & Blattner, F.R. (2013b) Molecular phylogenetics and morphological evolution of St. John's wort (*Hypericum*; Hypericaceae). *Molecular Phylogenetics and Evolution*, 66, 1–16.

Nürk, N.M., Uribe-Convers, S., Gehrke, B., Tank, D.C. & Blattner, F.R. (2015) Oligocene niche shift, Miocene diversification - Cold tolerance and accelerated speciation rates in the St. John's Worts (*Hypericum*, Hypericaceae). *BMC Evolutionary Biology*, 15, 1–13.

Rutter, N., Coronato, A., Helmens, K., Rabassa, J. & Zarate, M. (2012) The Glacial Record of Northern South America. *Glaciations in North and South America from the Miocene to the Last Glacial Maximum. Comparisons, linkages, and incertainties* (ed. by N. Rutter, A. Coronato, K. Helmens, J. Rabassa and M. Zarate), pp. 25–34. Springer Netherlands.

Taberlet, P., Gielly, L., Pautou, G. & Bouvet, J. (1991) Universal primers for amplification of three non-coding regions of chloroplast DNA. *Plant molecular biology*, 17, 1105–1109.

Torres, V., Hooghiemstra, H., Lourens, L. & Tzedakis, P.C. (2013) Astronomical tuning of long pollen records reveals the dynamic history of montane biomes and lake levels in the tropical high Andes during the Quaternary. *Quaternary Science Reviews* 63, 59–72.

Van der Hammen, T., Werner, J.H. & Van Dommelen, H. (1973) Palynological record of the upheaval of the northern Andes: a study of the Pliocene and Lower Quaternary of the Colombian eastern Cordillera and the early evolution of its high-Andean biota. *Review of Palaeobotany and Palynology*, 16, 1–122.